Prion Diseases and Emerging Prion Diseases

Takashi Yokoyama* and Shirou Mohri

Prion Disease Research Center, National Institute of Animal Health, 3-1-5 Kannondai, Tsukuba, Ibaraki 305-0856, Japan

Abstract: Transmissible spongiform encephalopathies (TSEs), also called prion diseases, are fatal neurodegenerative disorders. An abnormal isoform of the prion protein (PrP^{Sc}) generated by post-translational modification of the cellular prion protein (PrP^{C}) is believed to be the main component of this infectious agent. PrP^{Sc} is relatively resistant to proteinase K (PK) digestion. This characteristic has been widely accepted as the physicochemical basis for distinguishing between PrP^{C} and PrP^{Sc}. PrP^{C} is a glycoprotein that contains 2 Asn-linked glycosylation sites; it is present in the cells in 3 different glycoforms, including an unglycosylated form. Hence, for different prion strains, PrP^{Sc} exhibits different glycoform patterns with different ratios of the 3 forms by western blot. Recently, phenotypes of TSEs have emerged that exhibit PrP^{Sc} with different glycoform patterns and/or mild PK resistance in comparison with previously described typical cases. Regarding sheep scrapie, atypical scrapie cases that are represented by Nor98 have been reported among sheep previously presumed to be genetically scrapie-resistant. Moreover, atypical bovine spongiform encephalopathy (BSE) cases have been reported. These are classified into 2 phenotypes (H-type and L-type) based on the molecular weight of unglycosylated band of PK-digested PrP^{Sc}. The origin of these emerging prion diseases is obscure, conformational differences of PrP^{Sc} may cause the different biological and biochemical characteristics of prion strains.

PRION DISEASES

Creutzfeldt-Jakob disease (CJD) in humans, bovine spongiform encephalopathy (BSE) in cattle, scrapie in sheep and goats, transmissible mink encephalopathy (TME), and chronic wasting disease (CWD) in deer and elk are also known as prion diseases or transmissible spongiform encephalopathies (TSEs) [1]. They are fatal neurodegenerative diseases, and the affected animals eventually die after long incubation periods. Spongiform changes and gliosis are observed as pathological changes in the brain without any inflammatory response. There is no available cure or, with the exception of BSE, a prevention strategy that will guarantee protection against these diseases. The nature of TSE agents (prions) has not been fully elucidated. A misfolded isoform of prion protein (PrP) named PrP^{Sc} is considered to be responsible for the diseases [1]. PrP^{Sc} deposition has been observed in diseased animal brains, lymphoid tissues and some other tissues. Recent evidence showing that a recombinant mouse PrP can be transformed to become infectious to mice lends credence to the "protein-only hypothesis" [2]. PrP^{Sc} comprises the main component of prions, and it is partially resistant to proteinase digestion [3]. Prions are highly resistant to heat, disinfectants, chemicals, and routine autoclaving treatment [4].

PrP^{C} AND PrP^{SC}

The nature of the prion has not been fully elucidated. PrP^{Sc} is generated by the post-translational modification of the cellular isoform of PrP (PrP^{C}), which is a cell membrane glycoprotein [5]. PrP^{C} is highly conserved and with a high degree of homology among many mammalian species. This is the cause of the interspecies transmissibility of prions. In contrast, some critical amino acid differences between animal species may interfere with prion transmissibility and cause a phenomenon known as the "species barrier" [6]. Although there is increasing evidence of a role for PrP^{C} in oxidative stress and neuronal calcium homeostasis, its true function has not yet been clarified [7]. The conversion of PrP^{C} to PrP^{Sc} is believed to be the central event in prion pathogenesis. Consequently, clarification of the role of PrP^{C} may enable a better understanding of the detailed pathogenesis of prion diseases. PrP^{Sc} is the only known disease-specific marker and is closely associated with infectivity. Conformational differences are observed between PrP^{C} and PrP^{Sc}. The latter has an enhanced β sheet content and diminution of the α-helical content as compared to the former [8-10]; hence, PrP^{Sc} is relatively resistant to protease digestion. The protease resistance of PrP^{Sc} has been widely accepted as the physicochemical basis for distinguishing between PrP^{C} and PrP^{Sc} by most research and diagnostic tools, although some alternative approaches have been developed. Prions may adopt multiple conformations within one strain, during the process of conversion from PrP^{C} to PrP^{Sc}. The existence of a proteinase K (PK)-sensitive PrP^{Sc} or an intermediate (immature) form of PrP^{Sc} is suspected [11]. The relationship between the conformation of PrP^{Sc} and transmissibility remains unclear. Further, because of its insolubility and property of aggregation, the conformation of PrP^{Sc} remains obscure. PrP^{Sc} derived from, or associated with, different strains may exhibit different degrees of PK resistance [12]. The emergence of atypical prion diseases together with the differing characteristics of PrP^{Sc}, such as atypical scrapie, questions the definition of PrP^{Sc}.

PRION STRAINS

It is known that scrapie prions comprise several strains that show different biological phenotypes (attack rate, incubation period, clinical signs and lesion profiles) in the same inbred mice [13]. It has been shown that the PrP^{Sc} profile (distribution pattern and descriptive characteristics of deposits) in such mice is distinct for each prion strain once stabilized through sub-passage. Although the molecular basis for strain variation remains unclear, according to the protein-only hypothesis, strain characteristics are encoded within different conformations or aggregated forms of PrP^{Sc}. It is well known that the 2 TME strains isolated from mink to hamsters produced different clinical symptoms and incubation periods along with the different PrP^{Sc} biochemical characteristics. The HY (hyper) strain causes overexcitement and ataxia, while the DY (drowsy) strain causes lethargy and ataxia without hyperesthesia [14-16]. BSE- and variant CJD (vCJD)-inoculated mice showed similar lesion profiles and incubation periods, which supported the relationship between these 2 diseases [17] although care is needed in over-interpreting incubation period data as other studies have shown significant variation between BSE isolates [18] presumed to be due to differences in infectivity levels in the source brains. Several biological parameters can be used to characterize PrP^{Sc} and associated strains, including PK resistance [12, 19], glycoform ratios (Fig. **1**) [20], molecular weight of PK-digested PrP^{Sc} [21, 22], and immunoreactivity following guanidine treatment [23]. Glycoform ratios and the molecular weight of PK-digested PrP^{Sc} also supported the relationship between BSE and vCJD [20].

PrP^{SC} GLYCOFORM

PrP^{C} is a glycoprotein and contains 2 Asn-linked glycosylation sites. It is present in cells in 3 different glycosylated forms (digly-

*Address correspondence to this author at the Prion Disease Research Center, National Institute of Animal Health, 3-1-5 Kannondai, Tsukuba, Ibaraki 305-0856, Japan; Tel/Fax: +81-29- 838-7757; E-mail: tyoko@affrc.go.jp

0929-8673/08 $55.00+.00

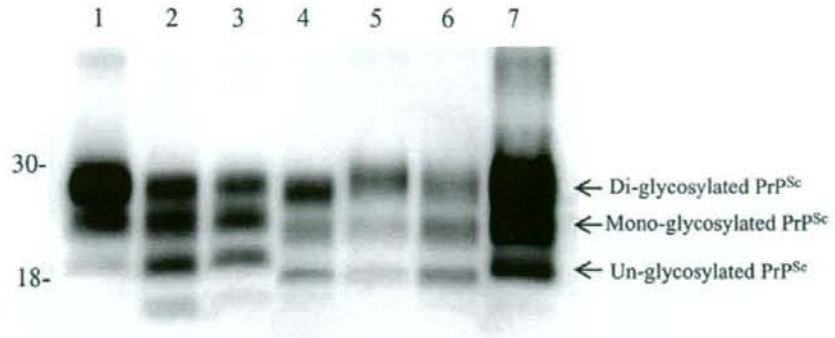

Fig. (1). Westernblot analysis of PrP^{Sc}. PrP^{Sc} was detected by anti-PrP antibody. Lanes: 1, scrapie Sc237 affected hamster; 2, scrapie Obihiro affected mouse; 3, scrapie RML affected mouse; 4, BSE affected mouse; 5, classical BSE affected cow; 6, atypical BSE affected cow (L-type); 7, scrapie affected sheep. Molecular markers are shown on the left (in kDa).

cosylated, monoglycosylated, and unglycosylated). It has been reported that PrP^{Sc} exhibits varying glycoform patterns, with different ratios of the 3 forms, when different prion strains are compared by western blotting (WB) (Fig. **1**) [20]. Analysis of the PrP^{Sc} glycoform ratio has been used to discriminate between prion strains and has gained increasing importance in the differential diagnosis of human prion diseases [24]. However, the molecular basis of strain-specific glycoform variability in prions, particularly in sheep scrapie, has remained elusive [25]. Clarifying the mechanism underlying PrP glycosylation might lead to the understanding of prion strain variations. It has been proposed that the PrP^{C} glycoform ratio varies between brain regions, and that differential targeting of neurons by prion strains results in the different PrP^{Sc} glycoform ratios [26, 27]. The PrP^{C} glycoforms are influenced by the amino acid sequence at PrP131-188 [28]. Furthermore, different scrapie prions can induce the formation of different PrP^{Sc} glycosylation patterns in the same cell line [29, 30]. These observations suggest that the direct influence of a prion strain on post-translational glycosylation modification of PrP^{C}, or on PrP^{Sc}, itself dictates strain-specific glycosylation [27-30].

PrP GENE AND SPECIES BARRIER

Transmission of prions between species is generally more difficult than within species, and this phenomenon, referred to as the species barrier, is expressed as prolonged incubation periods and/or less efficient transmissibility (lower attack rate) [6]. The confirmation of transmission is usually based on the onset of clinical disease and the detection of PrP^{Sc} accumulation in the central nervous system (CNS) at the end of the experiment, although in some circumstances clinical disease may not be apparent [31]. Although the precise mechanism or resistance has not yet been elucidated, it is believed to be due to differences in the amino acid sequences of PrP^{Sc} in the inoculum and PrP^{C} expressed in the recipient animal [32]. The murine PrP gene exists in 2 allelic forms with 2 amino acid substitutions (L108F and T189V), and these differences are responsible for the different incubation periods of prion diseases [33]. It is generally accepted that the susceptibility of sheep to scrapie is directly linked to the particular allelic polymorphisms of PrP. Sheep carrying alleles encoding VRQ or ARQ at amino acid positions 136, 154, and 171 of PrP are highly susceptible, although not necessarily to the same strains, whereas those carrying alleles encoding ARR appear to have protection against classical sheep scrapie but not against atypical scrapie. There is, however, a need to take into account the route and dose of infection, as well as the age as challenge, and in such circumstances it is clear that resistance to experimental challenge may not be absolute, to classical scrapie or BSE [34-36]. In addition to the PrP gene, other factors, including the concentration of PrP^{C} in the recipient animal [37], level of PK-sensitive PrP^{Sc} [23], and unidentified host-specific factors, such as the provisionally designated protein X [38, 39], have been shown to modify the incubation periods in prion diseases.

SCRAPIE IN SHEEP AND GOATS

Scrapie in sheep and goats is the longest known and most widespread disease form of TSEs. Its world-wide occurrence in indigenous sheep has been recognized for more than 2 centuries, especially in Europe although Australia, New Zealand and Argentina appear to remain free. The status of many countries is however, unknown because of the lack of sufficient surveillance.

PrP^{Sc} accumulates in the CNS at the middle to later stages of incubation. In scrapie-affected sheep, PrP^{Sc} can be detected both in the CNS and lymphoid tissues, although this is influenced by the PrP genotype of the animal. Where there is a peripheral distribution of PrP^{Sc} it can be demonstrated to accumulate in lymphoid tissues before deposition in the CNS, and it can thus be used for the antemortem diagnosis of sheep scrapie. However, even among sheep with identical PrP genotypes, the accumulation of PrP^{Sc} in the palatine tonsils in natural scrapie cases [40] can be variable. Attempts have been made to classify sheep scrapie prion strains, the scale of characterization internationally has been small. Although scrapie is believed to be the origin of BSE, a BSE-like scrapie strain has not yet been detected. The absence of clinically affected animals in certain genotypes of sheep led to the belief that they were genetically resistant to classical sheep scrapie. Despite uncertainty regarding whether the resistance was absolute, or simply prevented onset of clinical disease, in the UK, France, and many EU countries, large-scale genotyping and breeding programs were initiated in order to increase the scrapie-resistant sheep population [41, 42]. This eradication strategy relies on the removal of sheep that are considered genetically susceptible and on the selective breeding of scrapie-resistant animals. This policy was however driven by a desire to minimize the risk of BSE-infection in genetically susceptible sheep, and thus offer a degree of consumer protection. There are however a limited number of reports of classical scrapie in genetically resistant sheep that suggest that the resistance is relative rather than absolute [43, 44].

ATYPICAL SCRAPIE

Recently, in Norway, a number of atypical cases of scrapie sheep were designated as atypical scrapie, Nor98 [45]. Similar atypical cases were also reported from other European countries following extensive surveillance [46-49]. Atypical scrapie differs from classical scrapie and BSE in several features, including the WB pattern and degree of PK resistance of PrP^{Sc}. PK digestion of

PrP^{Sc} from Nor98 cases generates smaller fragments with molecular weights of 7 kDa (Nor98-PrP7; PrP85-148) and 14 kDa (PrP-CTF14; PrP120-233) [50, 51]. In these cases, less-stable PrP^{Sc} conformers coexist with PrP core amyloid [45-47]. Under mild PK conditions, PrP^{Sc} from atypical scrapie presents a diffuse banding pattern similar to undigested PrP^{C}. However, under stringent PK conditions, PrP^{Sc} is completely destroyed., and although some cases could not initially be confirmed by immunohistochemistry [52] and methods have been re-optimised to enable detection [45]. Furthermore, atypical scrapie mainly affects sheep that were previously believed to be genetically resistant to scrapie [48], in particular, sheep with AFRQ/AFRQ (136, 141, 154, and 171); AHQ/AHQ (136, 154, and 171); and AFRQ/AHQ genotypes [53, 54]. The occurrence of atypical scrapie in ARR/ARR sheep that were selected to generate scrapie-resistant flocks cautions against the aim of the genetic selection program to generate such flocks where the risk of BSE is low. Atypical scrapie is transmissible to ovinized transgenic mice [55]. Biochemical and transmission studies in mice have demonstrated that these cases may be attributable to a unique agent, but such evidence is not yet conclusive.

BSE

BSE was first recognized in the UK [56], and the epizootic has been demonstrated to be due to the consumption of proprietary concentrates or feed supplements contaminated with BSE prions [57]. The recognition of the relationship between BSE and vCJD raised consumer concerns regarding food safety. In recent years cases of BSE have been reported in most of Europe, North America, and Japan. The BSE incidence is however declining because of bans on the feeding of meat and bone meal to cattle that are in place in affected countries. The experimental transmissibility of BSE to cattle and other animals has been previously demonstrated. The uniform pathology among BSE-affected cattle, and consistent but limited results obtained after the experimental transmission of BSE to mice led to the belief that BSE was caused by a single prion strain. Both BSE and its human counterpart, vCJD, have been associated with a single prion strain [17, 58]. This strain is characterized by a unique and remarkably stable biochemical profile of PrP^{Sc} isolated from the brains of affected animals or humans [20]. The primary passage of BSE prions to different lines of inbred mice resulted in the isolation of 2 different prion strains with distinct PrP^{Sc} types, incubation periods, and PrP^{Sc} deposition patterns in the mouse brains [59]. BSE was widely transmitted to different animal species either naturally or experimentally. The risk of natural transmission of BSE to sheep and goats has prompted assessment of risk, and experimental investigation [60, 61]. The crucial involvement of the host genome may modulate prion strain selection and/or propagation in animals and it shows the possibility of the emergence of a novel prion strain during animal transmission. Several commercial diagnostic kits are available and used in surveillance programs for BSE. Most are based on the immunological detection of the PK-resistant PrP in its PrP^{Sc} form. Large scale surveillance and consequent biochemical analysis of PrP^{Sc} in positive samples has led to the detection of atypical BSE cases.

ATYPICAL BSE

Recently, different phenotypes among BSE cases in cattle have been reported in Japan, Europe, and North America and are designated as atypical BSE [62-65]. The transmissibility of some of the atypical BSE cases has been confirmed [66-69]. Currently, atypical BSE cases are classified into 2 groups, namely, the L-type and H-type, based on the molecular weight, glycoform ratio, and antibody binding characteristics of PK-digested PrP^{Sc}. The H-type is characterized by a significantly higher molecular mass of the unglycosylated band, but a conventional glycopattern, whereas the L-type PrP^{Sc} has a slightly lower molecular mass for the unglycosylated band and a distinctly different glycopattern. In limited examinations of whole brains, the L-type BSE had a different pattern of distribution and topology of PrP^{Sc} with PrP-immunopositive amyloid plaques, and was designated as bovine amyloidotic spongiform encephalopathy (BASE) [62]. Immunohistochemistry of the medulla oblongata is usually used for the diagnosis of classical BSE, but this approach in isolation is insufficient to discriminate between atypical and classical BSE. Whole brain and/or biochemical analysis of PrP^{Sc} is necessary to classify the BSE phenotype. A transmission study that used transgenic mice expressing bovine PrP confirmed the transmissibility of these 2 atypical BSE cases [66]. Transgenic bovinized mice are more susceptible to L-type than to classical BSE [66]. In addition, H-type BSE produced longer incubation periods than classical BSE, and showed a distinct phenotype, in transgenic bovinized XV mice [66, 69]. In addition, one study demonstrated the conversion of BASE to a phenotype indistinguishable from classical BSE following transmission *via* wild-type mice [69]. Limited information is available regarding atypical BSE, and its origins are still obscure.

In Japan, 2 atypical BSE cases have been reported. One case was of a 23-month-old steer (BSE/JP8) [63], and the other, a 14-year-old Japanese black (BSE/JP24) [70]. Although BSE/JP24 showed certain similar characteristics to BASE (an Italian case), the molecular weight of PrP^{Sc} in this case resembled that in classical BSE cases. This characteristic differs from BASE cases [70]; therefore, the identity and/or difference of these 2 atypical cases should be discussed carefully.

vCJD

Prior to the occurrence of BSE, no link was observed between animal and human prion diseases. BSE is the only concrete example of prion transmission to humans from another species [71]. The UK government banned the consumption by humans of certain tissues, perceived as being of high risk, and now called specified risk materials, in 1989, before the surge of BSE in cattle [72]. At that time, no rapid commercial tests were available, and diagnosis of BSE was thus based on a combination of clinical signs and histopathology. In spite of these measures, it was inevitable that cattle with preclinical BSE would have been consumed before the introduction of the ban. The epidemic of vCJD in the UK appears to be on the decline [73], and it is interesting that none have so far been identified that were born after the ban on consumption of specified risk materials. Cases of clinical vCJD are so far limited to patients with the 129MM genotype, but it remains to be seen whether a second wave of vCJD cases with longer incubation periods will occur in 129MV or 129VV genotypes. The human population exposed to BSE has a much more diverse genetic background than laboratory animals and/or cattle. An attempt to transmit BSE prions to humanized mice that express human PrP was unsuccessful [74]. Factors other than PrP genotype, so far unidentified, may also influence the susceptibility of humans to BSE prions, and may explain the surprisingly small epidemic of vCJD arising from the massive exposure of British consumers before 1989. However, it is known that human-to-human vCJD transmission occurs *via* blood transfusions [75, 76]. Caution therefore needs to be exercised in order to prevention the subsequent spread of vCJD between humans, in the absence of any species barrier.

PREVENTION OF PRION DISEASES

For animal prion diseases, prevention and control programs are based on an understanding of the epidemiology of the specific diseases, the introduction of specific measures to prevent subsequent transmission, such as feed bans for livestock, removal and destruction of specified offals to protect animals and humans, and the application of surveillance using post mortem BSE/TSE tests to confirm that the protective measures are working. For BSE, recom-

mendations are made by World Health Organization (WHO) and the World Organization for Animal Health (OIE) for the worldwide BSE eradication.

In human prion diseases, attempts to develop medical treatments and prevention are seriously challenged by the lack of understanding of the basic biology of prions. Several potential anti-prion drugs, such as amphotericin B [77], quinacrine [78], acridine [79], pentsan polysulfate (PPS) [80] are known to prolong incubation periods in prion-affected animals or to inhibit the formation of PrP^{Sc} in cultured cells. PPS and other sulfated polysaccharides are believed to work by inhibition of the conversion of PrP^{C} [81] or reducing PrP^{C} on the cell surface through stimulation of endocytosis [82] with a consequent therapeutic effect. Recently, PPS treatment has been evaluated through clinical trials involving CJD patients. For the treatment of prion disease, the compounds must be able to cross the blood-brain barrier in order to specifically target brain tissue, and the therapeutic effect of the compounds must be beyond the prion strains.

EMERGING PRION DISEASES

Prions were believed to consist of PrP^{Sc} alone. However, the existence of different strains and biological phenotypes contradicts the protein-only hypothesis. The recent recognition of atypical scrapie and atypical BSE, has complicated interpretation of data and the definition of prions. It is known that both host and prion characteristics influence prion pathogenesis. PrP^{Sc} in bovines with BSE or atypical BSE is no longer restricted to one strain, so it may be possible that additional phenotypes vCJD, with different PrP^{Sc} types, incubation periods, and neuropathology may still be recognized if the variant strains are transmissible to human. Risk assessments in relation to atypical BSE and atypical scrapie are necessary for food and/or medical safety. For this purpose, further scientific knowledge should be obtained regarding these emerging prion diseases. Furthermore, it has been reported that the virulence of BSE prions was enhanced by crossing the species barrier [83], raising the prospect that BSE that has transferred to other species may prove to be a greater risk to consumers than BSE in cattle, but this hypothesis remains to be proven. Studies regarding the transmission barrier are important with respect to the safety of the human food supply. The need for risk analyses of newly emerged prion diseases should be carefully considered. Further scientific knowledge regarding emerging prion diseases is necessary to ensure that the control of animal and human prion diseases is possible.

ACKNOWLEDGEMENT

We thank to Dr. Danny Matthews for reviewing the manuscript.

REFERENCES

[1] Prusiner, S.B. *Science*, **1991**, *252*, 1515.
[2] Legname, G.; Baskakov, I.V.; Nguyen, H.-O.B.; Riesner, D.; Cohen, F.E.; DeArmond, S.J.; Prusiner, S.B. *Science*, **2004**, *305*, 673.
[3] McKinley, M.P.; Bolton, D.C.; Prusiner, S.B. *Cell*, **1983**, *35*, 57.
[4] Rohwer, R.G. In *Curr. Top. Microbiol. Immunol.*, **1991**, *172*, 195.
[5] Oesch, B.; Westaway, D.; Wälchli, M.; McKinley, M.P.; Kent, S.B.H.; Aebersold, R.; Barry, R.A.; Tempst, P.; Teplow, D.B.; Hood, L.E.; Prvsiner, S.B.; Weissmann, C. *Cell*, **1985**, *40*, 735.
[6] Kimberlin, R.H. In *Sub-acute spongiform encephalopathies*. Bradley, R.; Savey, M.; Marchant, B., Eds.; Kluwer Academic Publishers: Dordrecht, **1991**, pp. 137.
[7] Herms, J.; Kretzschmar, H. In *Prions in humans and animals*. Hornlimann, B.; Riesner, D.; Kretzschmar, H. Eds.; Walter de Gruyter: Berlin, **2006**, pp. 95.
[8] Caughey, B.; Raymond, G.J. *J. Biol. Chem.*, **1991**, *266*, 18217.
[9] Pan, K.-M.; Baldwin, M.; Nguyen, J.; Gasset, M.; Serban, A.; Groth, D.; Mehlhorn, I.; Huang, Z.; Fletterick, R.J.; Cohen, F.E.; Prvsiner, S.B. *Proc. Natl. Acad. Sci. USA*, **1993**, *90*, 10962.
[10] Safar, J.; Roller, P.P.; Gajdusek, D.C.; Gibbs, C.J., Jr. *Protein Sci.*, **1993**, *2*, 2206.
[11] Safar, J.G.; Geschwind, M.D.; Deering, C.; Didorenko, S.; Sattavat, M.; Sanchez, H.; Serban, A.; Vey, M.; Baron, H.; Giles, K.; Miller, B.L.; Dearmond, S.J.; Prusiner, S.B. *Proc. Natl. Acad. Sci. USA*, **2005**, *102*, 3501.
[12] Kuczius, T.; Groschup, M.H. *Mol. Med.*, **1999**, *5*, 406.
[13] Bruce, M.E. In *Prion diseases*. Baker, H.F.; Ridley, R.M. Eds.; Human Press: Totowa, **1996**, pp. 223.
[14] Bessen, R.A.; Marsh, R.F. *J. Virol.*, **1992**, *66*, 2096.
[15] Bessen, R.A.; Marsh, R.F. *J. Gen. Virol.*, **1992**, *73*, 329.
[16] Bessen, R.A.; Marsh, R.F. *J. Virol.*, **1994**, *68*, 7859.
[17] Bruce, M.E.; Will, R.G.; Ironside, J.W.; McConnell, I.; Drummond, D.; Suttie, A.; McCardle, L.; Chree, A.; Hope, J.; Birkett, C.; Cousens, S.; Fraser, H.; Bostock, C.J. *Nature*, **1997**, *389*, 498.
[18] Green, R.; Horrocks, C.; Wilkinson, A.; Hawkins, S.A.C.; Ryder, S.J. *J. Comp. Pathol.*, **2005**, *132*, 117.
[19] Kascsak, R.J.; Rubenstein, R.; Merz, P.A.; Carp, R.I.; Wisniewski, H.M.; Diringer, H. *J. Gen. Virol.*, **1985**, *66*, 1715.
[20] Collinge, J.; Sidle, K.C.L.; Meads, J.; Ironside, J.; Hill, A.F. *Nature*, **1996**, *383*, 685.
[21] Rubenstein, R.; Merz, P.A.; Kascsak, R.J.; Carp, R.I.; Scalici, C.L.; Fama, C.L.; Wisniewski, H.M. *J. Infect. Dis.*, **1987**, *156*, 36.
[22] Hayashi, H.K.; Yokoyama, T.; Takata, M.; Iwamaru, Y.; Imamura, M.; Ushiki, Y.K.; Shinagawa, M. *Biochem. Biophys. Res. Commun.*, **2005**, *328*, 1024.
[23] Safar, J.; Wille, H.; Itri, V.; Groth, D.; Serban, H.; Torchia, M.; Cohen, F.E.; Prusiner, S.B. *Nat. Med.*, **1998**, *4*, 1157.
[24] Zanusso, G.; Farinazzo, A.; Fiorini, M.; Gelati, M.; Castagna, A.; Righetti, P.G.; Rizzuto, N.; Monaco, S. *J. Biol. Chem.*, **2001**, *276*, 40377.
[25] Hope, J.; Wood, S.C.E.R.; Birkett, C.R.; Chong, A.; Bruce, M.E.; Cairns, D.; Goldmann, W.; Hunter, N.; Bostock, C.J. *J. Gen. Virol.*, **1999**, *80*, 1.
[26] DeArmond, S.J.; Qiu, Y.; Sánchez, H.; Spilman, P.R.; Ninchak-Casey, A.; Alonso, D.; Daggett, V. *J. Neuropathol. Exp. Neurol.*, **1999**, *58*, 1000.
[27] Somerville, R.A. *J. Gen. Virol.*, **1999**, *80*, 1865.
[28] Yokoyama, T.; Shimada, K.; Masujin, K.; Iwamaru, Y.; Imamura, M.; Ushiki, Y.K.; Kimura, K.M.; Itohara, S.; Shinagawa, M. *Arch. Virol.*, **2007**, *152*, 603.
[29] Birkett, C.R.; Hennion, R.M.; Bembridge, D.A.; Clarke, M.C.; Chree, A.; Bruce, M.E.; Bostock, C.J. *EMBO J.*, **2001**, *20*, 3351.
[30] Vorberg, I.; Priola, S.A. *J. Biol. Chem.*, **2002**, *277*, 36775.
[31] Hill, A.F.; Joiner, S.; Linehan, J.; Desbruslais, M.; Lantos, P.L.; Collinge, J. *Proc. Natl. Acad. Sci. USA*, **2000**, *97*, 10248.
[32] Scott, M.R.; Groth, D.; Tatzelt, J.; Torchia, M.; Tremblay, P.; DeArmond, S.J.; Prusiner, S.B. *J. Virol.*, **1997**, *71*, 9032.
[33] Westaway, D.; Goodman, P.A.; Mirenda, C.A.; McKinley, M.P.; Carlson, G.A.; Prusiner, S.B. *Cell*, **1987**, *51*, 651.
[34] Baron, T.G.M.; Madec, J.-Y.; Calavas, D.; Richard, Y.; Barillet, F. *Neurosci. Lett.*, **2000**, *284*, 175.
[35] Cordier, C.; Benestk, A.; Philippe, S.; Bètemps, D.; Ronzon, F.; Calavas, D.; Crozet, C.; Baron, T. *J. Gen. Virol.*, **2006**, *87*, 3763.
[36] Houston, E.F.; Gravenor, M.B. *Vet. Rec.*, **2003**, *152*, 333.
[37] Prusiner, S.B.; Scott, M.; Foster, D.; Pan, K.-M.; Groth, D.; Mirenda, C.; Torchia, M.; Yang, S.-L.; Serban, D.; Carlson, G.A.; Hoppe, P.C.; Westaway, D.; De Armond, S.J. *Cell*, **1990**, *63*, 673.
[38] Telling, G.C.; Scott, M.; Mastrianni, J.; Gabizon, R.; Torchia, M.; Cohen, F.E.; DeArmond, S.J.; Prusiner, S.B. *Cell*, **1995**, *83*, 79.
[39] Kaneko, K.; Zulianello, L.; Scott, M.; Cooper, C.M.; Wallace, A.C.; James, T.L.; Cohen, F.E.; Prusiner, S.B. *Proc. Natl. Acad. Sci. USA*, **1997**, *94*, 10069.
[40] Shimada, K.; Hayashi, H.K.; Ookubo, Y.; Iwamaru, Y.; Imamura, M.; Takata, M.; Schmerr, M.J.; Shinagawa, M.; Yokoyama, T. *Microbiol. Immunol.*, **2005**, *49*, 801.
[41] Arnold, M.; Meek, C.; Webb, C.R.; Hoinville, L.J. *Prev. Vet. Med.*, **2002**, *56*, 227.
[42] Dawson, M.; Hoinville, L.J.; Hosie, B.D.; Hunter, N. *Vet. Rec.*, **1998**, *142*, 623.
[43] Ikeda, T.; Horiuchi, M.; Ishiguro, N.; Muramatsu, Y.; Kai-Uwe, G.D.; Shinagawa, M. *J. Gen. Virol.*, **1995**, *76*, 2577.
[44] Groschup, M.H.; Lacroux, C.; Buschmann, A.; Lühken, G.; Mathey, J.; Eiden, M.; Lugan, S.; Hoffmann, C.; Espinosa, J.C.; Baron, T.; Torres, J.M.; Erhardt, G.; Andreoletti, O. *Emerg. Infect. Dis.*, **2007**, *13*, 1201.
[45] Benestad, S.L.; Sarradin, P.; Thu, B.; Schönheit, J.; Tranulis, M.A.; Bratberg, B. *Vet. Rec.*, **2003**, *153*, 202.
[46] Onnasch, H.; Gunn, H.M.; Bradshaw, B.J.; Benestad, S.L.; Bassett, H.F. *Vet. Rec.*, **2004**, *155*, 636.
[47] Gavier-Widén, D.; Nöremark, M.; Benestad, S.; Simmons, M.; Renström, L.; Bratberg, B.; Elvander, M.; af Segerstad, C.H. *J. Vet. Diagn. Invest.*, **2004**, *16*, 562.
[48] Buschmann, A.; Lühken, G.; Schultz, J.; Erhardt, G.; Groschup, M.H. *J. Gen. Virol.*, **2004**, *85*, 2727.
[49] Konold, T.; Davis, A.; Bone, G.; Bracegirdle, J.; Everitt, S.; Chaplin, M.; Saunders, G.C.; Cawthraw, S.; Simmons, M.M. *BMC Vet. Res.*, **2007**, *3*, 2.
[50] Gretzschel, A.; Buschmann, A.; Langeveld, J.; Groschup, M.H. *J. Gen. Virol.*, **2006**, *87*, 3715.
[51] Klingeborn, M.K.; Wik, L.; Simonsson, M.; Renström, L.H.M.; Ottinger, T.; Linné, T. *J. Gen. Virol.*, **2006**, *87*, 1751.

[52] Everest, S.J.; Thorne, L.; Barnicle, D.A.; Edwards, J.C.; Elliott, H.; Jackman, R.; Hope, J. *J. Gen. Virol.*, **2006**, *87*, 471.
[53] Saunders, G.C.; Cawthraw, S.; Mountjoy, S.J.; Hope, J.; Windl, O. *J. Gen. Virol.*, **2006**, *87*, 3141.
[54] Lühken, G.; Buschmann, A.; Brandt, H.; Eiden, M.; Groschup, M.H.; Erhardt, G. *Vet. Res.*, **2007**, *38*, 65.
[55] Le Dur, A.; Béringue, V.; Andréoletti, O.; Reine, F.; Laï, T.L.; Baron, T.; Bratberg, B.; Vilotte, J.-L.; Sarradin, P.; Benestad, S.L.; Laude, H. *Proc. Natl. Acad. Sci. USA*, **2005**, *102*, 16031.
[56] Wells, G.A.H.; Scott, A.C.; Johnson, C.T.; Gunning, R.F.; Hancock, R.D.; Jeffrey, M.; Dawson, M.; Bradley, R. *Vet. Rec.*, **1987**, *121*, 419.
[57] Wells, G.A.H.; Wilesmith, J.W. *Brain Pathol.*, **1995**, *5*, 91.
[58] Hill, A.F.; Desbruslais, M.; Joiner, S.; Sidle, K.C.L.; Gowland, I.; Collinge, J.; Doey, L.J.; Lantos, P. *Nature*, **1997**, *389*, 448, 526.
[59] Lloyd, S.E.; Linehan, J.M.; Desbruslais, M.; Joiner, S.; Buckell, J.; Brandner, S.; Wadsworth, J.D.F.; Collinge, J. *J. Gen. Virol.*, **2004**, *85*, 2471.
[60] Bellworthy, S.J.; Dexter, G.; Stack, M.; Chaplin, M.; Hawkins, S.A.C.; Simmons, M.M.; Jeffrey, M.; Martin, S.; Gonzalez, L.; Hill, P. *Vet. Rec.*, **2005**, *157*, 206.
[61] Schreuder, B.E.C.; Somerville, R.A. *Rev. Sci. Tech.*, **2003**, *22*, 103.
[62] Casalone, C.; Zanusso, G.; Acutis, P.; Ferrari, S.; Capucci, L.; Tagliavini, F.; Monaco, S.; Caramelli, M. *Proc. Natl. Acad. Sci. USA*, **2004**, *101*, 3065.
[63] Yamakawa, Y.; Hagiwara, K.; Nohtomi, K.; Nakamura, Y.; Nishijima, M.; Higuchi, Y.; Sato, Y.; Sata, T.; the expert committee for BSE diagnosis, Ministry of Health, Labour and Welfare of Japan. *Jpn. J. Infect. Dis.*, **2003**, *56*, 221.
[64] Bracabe, A.-G.; Laplanche, J.-L.; Ryder, S.; Baron, T. *EMBO Rep.*, **2004**, *5*, 110.
[65] Jacobs, J.G.; Langeveld, J.P.M.; Biacabe, A.-G.; Acutis, P.-L.; Polak, M.P.; Gavier-Widen, D.; Buschmann, A.; Caramelli, M.; Casalone, C.; Mazza, M.; Groschup, M.; Erkens, J.H.F.; Davidse, A.; van Zijderveld, F.G.; Baron, T. *J. Clin. Microbiol.*, **2007**, *45*, 1821.
[66] Buschmann, A.; Gretzschel, A.; Biacabe, A.-G.; Schiebel, K.; Corona, C.; Hoffmann, C.; Eiden, M.; Baron, T.; Casalone, C.; Groschup, M.H. *Vet. Microbiol.*, **2006**, *117*, 103.
[67] Baron, T.; Biacabe, A.-G.; Arsac, J.-N.; Benestad, S.; Groschup, M.H. *Vaccine*, **2007**, *25*, 5625.
[68] Béringue, V.; Bencsik, A.; Le Dur, A.; Reine, F.; Laï, T.L.; Chenais, N.; Tilly, G.; Biacabé, A.-G.; Baron, T.; Vilotte, J.-L.; Laude, H. *PLoS Pathog.*, **2006**, *2*, e112.
[69] Capobianco, R.; Casalone, C.; Suardi, S.; Mangieri, M.; Miccolo, C.; Limido, L.; Catania, M.; Rossi, G.; Di Fede, G.; Giaccone, G.; Bruzzone, M.G.; Minati, L.; Corona, C.; Acutis, P.; Gelmetti, D.; Lombardi, G.; Groschup, M.H.; Buschmann, A.; Zanusso, G.; Monaco, S.; Caramelli, M.; Tagliavini, F. *PLoS Pathog.*, **2007**, *3*, e31.
[70] Hagiwara, K.; Yamakawa, Y.; Sato, Y.; Nakamura, Y.; Tobiume, M.; Shinagawa, M.; Sata, T. *Jap. J. Inf. Dis.*, **2007**, 60, 305.
[71] Groschup, M.H.; Hörnlimann, B.; Buschmann, A. In *Prions in humans and animals*. Hörnlimann, B.; Riesner, D.; Kretzschmar, H. Eds.; Walter de Gruyter: Berlin, **2006**, pp. 483.
[72] Wilesmith, J.W.; Ryan, J.B.M.; Atkinson, M.J. *Vet. Rec.*, **1991**, *128*, 199.
[73] Manson, J.C.; Cancellotti, E.; Hart, P.; Bishop, M.T.; Barron, R.M. *Biochem. Soc. Trans.*, **2006**, *34*, 1155.
[74] Bishop, M.T.; Hart, P.; Aitchison, L.; Baybutt, H.N.; Plinston, C.; Thomson, V.; Tuzi, N.L.; Head, M.W.; Ironside, J.W.; Will, R.G.; Manson, J.C. *Lancet Neurol.*, **2006**, *5*, 393.
[75] Llewelyn, C.A.; Hewitt, P.E.; Knight, R.S.G.; Amar, K.; Cousens, S.; Mackenzie, J.; Will, R.G. *Lancet*, **2004**, *363*, 417.
[76] Peden, A.H.; Head, M.W.; Ritchie, D.L.; Bell, J.E.; Ironside, J.W. *Lancet*, **2004**, *364*, 527.
[77] McKenzie, D.; Kaczkowski, J.; Marsh, R.; Aiken, J. *J. Virol.*, **1994**, *68*, 7534.
[78] Yung, L.; Huang, Y.; Lessard, P.; Legname, G.; Lin, E.T.; Baldwin, M.; Prusiner, S.B.; Ryou, C.; Guglielmo, B.J. *BMC Infect. Dis.*, **2004**, *4*, 53.
[79] Korth, C.; May, B.C.H.; Cohen, F.E.; Prusiner, S.B. *Proc. Natl. Acad. Sci. USA*, **2001**, *98*, 9836.
[80] Caughey, B.; Raymond, G.J. *J. Virol.*, **1993**, *67*, 643.
[81] Caughey, B.; Brown, K.; Raymond, G.J.; Katzenstein, G.E.; Thresher, W. *J. Virol.*, **1994**, *68*, 2135.
[82] Shyng, S.-L.; Lehmann, S.; Moulder, K.L.; Harris, D.A. *J. Biol. Chem.*, **1995**, *270*, 30221.
[83] Espinosa, J.C.; Andréoletti, O.; Castilla, J.; Herva, M.E.; Morales, M.; Alamillo, E.; San-Segundo, F.D.; Lacroux, C.; Lugan, S.; Salguero, F.J.; Langeveld, J.; Torres, J.M. *J. Virol.*, **2007**, *81*, 835.

Received: November 02, 2007 **Revised: February 10, 2008** **Accepted: February 11, 2008**

FULL PAPER *Virology*

Conformational Change in Hamster Scrapie Prion Protein (PrP27–30) Associated with Proteinase K Resistance and Prion Infectivity

Sachiko Y. SUZUKI[1)], Masuhiro TAKATA[1)], Kenta TERUYA[2)], Morikazu SHINAGAWA[1)], Shirou MOHRI[1)] and Takashi YOKOYAMA[1)]*

[1)]*Prion Disease Research Center, National Institute of Animal Health, Ibaraki 305–0856 and* [2)]*Division of Prion Biology, Department of Prion Research, Tohoku University Graduate School of Medicine, Sendai 980–8575, Japan*

(Received 28 May 2007/Accepted 9 October 2007)

ABSTRACT. The scrapie prion protein (PrP27–30) is a crucial component of the prion and is responsible for its transmissibility. Structural information on this protein is limited because it is insoluble and shows aggregated properties. In this study, PrP27–30 was effectively dispersed using sonication under the weak alkaline condition. Subsequently, the small PrP27–30 aggregates were subjected to different pH, heat, and denaturing conditions. The loss of proteinase K (PK) resistance of PrP27–30 and prion infectivity were monitored along with spectroscopic changes. Prion inactivation could not be achieved by the loss of PK resistance alone; a significant loss of the PrP27–30 amyloid structure, which was represented by a decrease in thioflavin T fluorescence, was required for the loss of transmissibility.

KEY WORDS: prion, small PrP27–30 aggregates, spectroscopic analysis, thioflavin T, transmissibility.

J. Vet. Med. Sci. 70(2): 159–165, 2008

The abnormal isoform of the prion protein (PrP^{Sc}) is the main component in the infectious agent that causes scrapie in sheep and goats and bovine spongiform encephalopathy in cattle. PrP^{Sc} differs from the normal cellular isoform of the prion protein (PrP^{C}) in its relative protease resistance [1, 13] and transmissibility [4, 12]. PrP^{Sc} is generated by the posttranslational modification of PrP^{C}, and this conformational change is considered to be the central event of pathogenesis of the prion. PrP^{Sc} is rich in β-sheets, while PrP^{C} is rich in α-helixes [2, 5]. However, the secondary and tertiary structures of PrP^{Sc} and the mechanisms underlying the conversion from PrP^{C} to PrP^{Sc} have not been elucidated in detail.

Although the spectroscopic structural analysis of proteins in solution has generally known to provide precise information at the molecular level, the process requires large amounts of highly purified samples. PrP^{Sc} is found in limited amounts in the brains of prion-affected animals, and the purified PrP^{Sc} fraction is contaminated with other proteins [17]. Due to these limitations, amyloid fibrils of synthetic peptide or recombinant prion protein (PrP) were subjected to analysis instead of PrP^{Sc}. However, the synthetic amyloid fibrils were not transmissible [8] and, hence, could not mimic authentic PrP^{Sc}.

The N-terminal region of PrP^{Sc} was truncated by enzymatic digestion under detergent conditions, and a component with an apparent molecular weight of 27,000 to 30,000 (PrP27–30) was generated. PrP27–30 was a highly purified fraction and exhibited transmissibility [15]. Structural analysis of PrP27–30 could provide information about the prion although it was artificially generated during the purification step [11]. PrP27–30 was analyzed by electron crystallography [23] and circular dichroism (CD) spectra of the dry film [18]. These analyses were performed using solid-state samples from which the water molecule was eliminated; therefore, these results might not reflect the precise conformation of PrP27–30 [14]. PrP27–30 in solid or solution states was analyzed by Fourier transform-infrared (FT-IR) spectra [21]. However, the FT-IR analysis only presented the secondary structural information.

Here, we prepared the small PrP27–30 aggregates in solution applicable for spectroscopic analysis. It showed proteinase K (PK) resistance and transmissibility. These characteristics were lost on treatment with alkali, heat, and denaturing agents. To analyze the correlation between the secondary and/or tertiary structures and the biological characteristics of PrP27–30, treated samples were analyzed by CD and fluorescence spectroscopy. The purpose of this study is to clarify the key structure of PrP27–30 that is related to prion transmissibility.

MATERIALS AND METHODS

Animals and prion: The hamster-passaged scrapie prion "Sc237" was intracerebrally inoculated into 3-week-old female Syrian hamsters (SLC, Japan) [24]. The hamsters were sacrificed during the terminal stages of their illness, and their brains were dissected and used for this study. Hamsters were also used in the incubation-period assay.

Purification and dispersion of PrP27–30: PrP27–30 was purified according to a previously reported procedure [22]. Briefly, 10 g of the brain samples was homogenized with 100 m*l* of 10 mM sodium-phosphate buffer (pH 7.4) containing 10% sarcosyl. The solution was then digested at room temperature for 1 hr using 25 unit/m*l* of benzonase. This digested sample was centrifuged at 22,000 *g* for 20 min. The supernatant was collected and centrifuged at 540,000 *g* for 30 min. The resulting pellet was suspended in

* CORRESPONDENCE TO: YOKOYAMA, T., Prion Disease Research Center, National Institute of Animal Health, 3–1–5 Kannondai, Tsukuba, Ibaraki 305–0856, Japan.
e-mail: tyoko@affrc.go.jp

10 m*l* of 10 mM sodium-phosphate buffer (pH 7.4) containing 1% sarcosyl and 10% NaCl and was then sonicated. The sample was treated with 100 μg/m*l* PK at 37°C for 1 hr, and the reaction was stopped by adding a final concentration of 1 mM phenylmethylsulfonyl fluoride. The sample was centrifuged at 22,000 *g* for 20 min, and the pellet was washed in 10 m*l* of 10 mM sodium-phosphate buffer (pH 7.4) by centrifugation at 22,000 *g* for 20 min. Next, the pellet was washed twice in 20 mM Tris-HCl buffer (pH 8.5) by centrifugation at 21,000 *g* for 30 min, resuspended in 5 m*l* of 20 mM Tris-HCl buffer (pH 8.5), and sonicated until the turbidity was cleared [20]. It was recentrifuged at 21,000 *g* for 30 min to obtain clear supernatant. The protein concentration of the supernatant was determined by using the BCA Protein Assay Kit (Pierce Biotechnology).

Incubation-period assay: The following treatment was performed under various denaturing conditions, and the samples were diluted to approximately 1:1,000 in phosphate-buffered saline (PBS). A 20-μ*l* aliquot containing approximately 0.4–0.8 *n*g of PrP27–30 was intracerebrally inoculated into hamsters. The clinical diagnosis of scrapie was confirmed by western blotting. The infectivity of PrP27–30 was determined according to a published procedure [16]. The procedure is based on the correlation between the titer and the incubation period.

Denaturation of PrP27–30: Under various denaturation conditions, 30–50 *ng*/μ*l* of the samples were incubated at 20°C for more than 12 hr. For pH treatment, the samples were incubated in buffers of varying pH (5.0–12.0); 50 mM sodium-acetic acid (pH 5.0), 25 mM sodium phosphate (pH 6.0, 7.0, and 12.0), 50 mM Tris-HCl (pH 8.0 and 9.0), 50 mM 3-(Cyclohexylamino)-1-propanesulfonic acid (CAPS; pH 10.0 and 11.0). For the treatment of varying denaturant concentrations, the samples were incubated in 20 mM Tris-HCl (pH 8.5) without denaturant and with 1.0, 2.0, and 4.0 M urea as well as with 1.0, 2.0, and 4.0 M guanidine HCl (GdnHCl). For heat treatment, the samples were incubated in 20 mM sodium-phosphate buffer (pH 8.5) for 30 min at 25°C, 65°C, and 100°C; they were then cooled at room temperature. The treated sample was subjected to spectroscopic analysis or subjected to PK digestion, as described below. No visible aggregation of PrP27–30 was observed after these treatments.

PK digestion of PrP27–30: Forty to fifty *ng*/μ*l* of the denatured sample was diluted 10 times by PBS and was digested at 37°C for 1 hr by mixing with an equal volume of 100 μg/m*l* PK in 100 mM Tris-HCl buffer (pH 7.0). The reaction was stopped by mixing with an equal volume of 2 × sodium dodecyl sulfate (SDS) sample buffer and then heated for 5 min at 100°C. The degree of PrP27–30 proteolysis was evaluated by the signal intensity of western blotting.

Western blotting: Western blotting was performed as previously described using the anti-PrP monoclonal antibody T2, and the blots were developed using a chemiluminescence substrate (Super Signal, Pierce Biotechnology) [7].

CD spectroscopy: CD was measured in a 1-mm path-length quartz cell using a spectropolarimeter (Model J-805; Jasco, Japan) at room temperature. The spectra were expressed as the mean residue ellipticity.

Fluorescence spectroscopy: The fluorescence spectra were determined using a spectrofluorometer (Model FP6300; Jasco, Japan) at 20°C. The intrinsic Trp fluorescence was measured at an excitation wavelength of 292 nm. 8-Amino-1-naphthalene sulfate (ANS) and thioflavin T (ThT) were added to the samples at a final concentration of 200 and 50 μM, respectively, and the respective excitation wavelengths were 380 and 444 nm.

RESULTS

Biochemical and biological properties of small PrP27–30 aggregates: The purified PrP27–30 was analyzed by silver staining and its purity was confirmed (data not shown). Approximately, 2.5 μg of small PrP27–30 aggregates were prepared from 1 g of diseased hamster brain. The small PrP27–30 aggregates showed resistance to PK digestion when treated at pH values ranging from 5.0 to 11.0 (Fig. 1A, lanes 1–7); however, it was digested by PK when treated at pH 12.0 (Fig. 1A, lane 8). Prion infectivity was also diminished by the treatment at pH 12.0 (Table 1). Heat treatment also diminished the PK resistance depending upon the increase in temperature (Fig. 1B, lanes 1–3). However, the decrease in infectivity was observed following treatment at 100°C (Table 1). PrP27–30 was slightly digested by PK on treatment with 4.0 M urea (Fig. 1C, lane 4), and was significantly digested by PK on treatment with 2.0 and 4.0 M GdnHCl (Fig. 1C, lanes 6, and 7). Although prion inactivation was observed with 4.0 M GdnHCl treatment, the infectivity was retained in the 4.0 M-urea-treated and 2.0 M-GdnHCl-treated samples (Table 1).

Spectroscopic analysis of small PrP27–30 aggregates

1) Secondary structural changes monitored by CD spectra: The CD spectra of PrP27–30 are shown in Fig. 2A–C. It formed the largest dichroic band approximately at 215 nm between pH 5.0 and 8.0, which is a characteristic of β-sheet rich proteins (Fig. 2A, black, blue, green, and yellow lines) [6]. The negative band was blue-shifted and increased at pH 9.0 and 10.0 (Fig. 2A, orange and red lines); however, the ellipticity decreased at pH 11.0 (Fig. 2A, grey line). In particular, the ellipticity at 200 nm and 215 nm decreased significantly at pH 12.0 (Fig. 2A, purple line). In heat treatment, the CD spectra revealed that the ellipticity at 215 nm was retained during treatment at 65°C (Fig. 2B, blue and yellow lines), while it decreased significantly during treatment at 100°C (Fig 2B, red line). In denaturant treatment, the ellipticity at 215 nm decreased gradually following an increase in urea or GdnHCl concentration (Fig. 2C).

2) Tertiary structural changes monitored by Trp fluorescence: The intrinsic Trp fluorescence intensity was used for the monitoring of protein structural fluctuations in tertiary structure. The Trp fluorescence increased under alkaline conditions (Fig. 2D). Between pH 5.0 and 9.0, the intensity at 345 nm was similar to that at 328 nm (Fig. 2D, black,

Fig. 1. PK digestion of PrP27–30 following treatment under different conditions. (A) PK digestion of PrP27–30 on treatment at different pH values. Lanes 1, 2, 3, 4, 5, 6, 7 and 8 represent the samples treated at pH 5.0, 6.0, 7.0, 8.0, 9.0, 10.0, 11.0, and 12.0, respectively. (B) PK digestion of PrP27–30 following treatment at different temperatures. Lanes 1, 2, and 3 represent the samples treated at 25°C, 65°C, and 100°C, respectively. (C) PK digestion of PrP27–30 following treatment with different urea or GdnHCl concentrations. Lane 1 represents the denaturant-untreated sample. Lanes 2, 3, and 4 represent the samples treated with 1.0, 2.0, and 4.0 M urea, respectively. Lanes 5, 6, and 7 represent the samples treated with 1.0, 2.0, and 4.0 M GdnHCl, respectively.

Table 1. Prion titers of small PrP27–30 aggregates treated under different conditions

Condition	PrP27–30 (*n*g)	No. of ill/ inoculated cases	Mean incubation ± SD (days)	Infectivity LD_{50}
pH 5.0	0.8	3/3	87 ± 0	4.4
pH 8.0	0.8	3/3	87 ± 0	4.4
pH 9.0	0.8	3/3	87 ± 0	4.4
pH 10.0	0.6	3/3	91 ± 1	4.0
pH 11.0	0.6	3/3	90 ± 2	4.1
pH 12.0	0.6	1/3	132	+[a]
25°C for 30 min	0.4	3/3	91 ± 7	4.0
65°C for 30 min	0.4	3/3	90 ± 2	4.1
100°C for 30 min	0.4	3/3	96 ± 1	3.5
no denaturant	0.6	2/2	90 ± 4	4.1
1.0 M urea	0.6	3/3	87 ± 0	4.4
4.0 M urea	0.6	3/3	99 ± 7	3.2
1.0 M GdnHCl	0.6	3/3	99 ± 9	3.2
2.0 M GdnHCl	0.6	3/3	108 ± 9	2.3
4.0 M GdnHCl	0.6	0/3	>290	–

[a] One of three hamsters was positive in PrP^{Sc}; however, the prion titer was not estimated by the incubation period assay.

blue, green, yellow, and orange lines). However, at pH 10.0–12.0, the intensity at 345 nm was slightly higher than that at 328 nm (Fig. 2D, red, grey, and purple lines). This indicated an increase in solvent-accessible Trp residues. With the heat treatment, the Trp fluorescence increased gradually (Fig. 2E). Corresponding to the denaturant concentration, the Trp fluorescence also increased gradually. Furthermore, the shoulder observed at 328 nm disappeared on treating PrP27–30 with 4.0 M urea and GdnHCl (Fig. 2F, green and yellow lines). This also demonstrated the signifi-

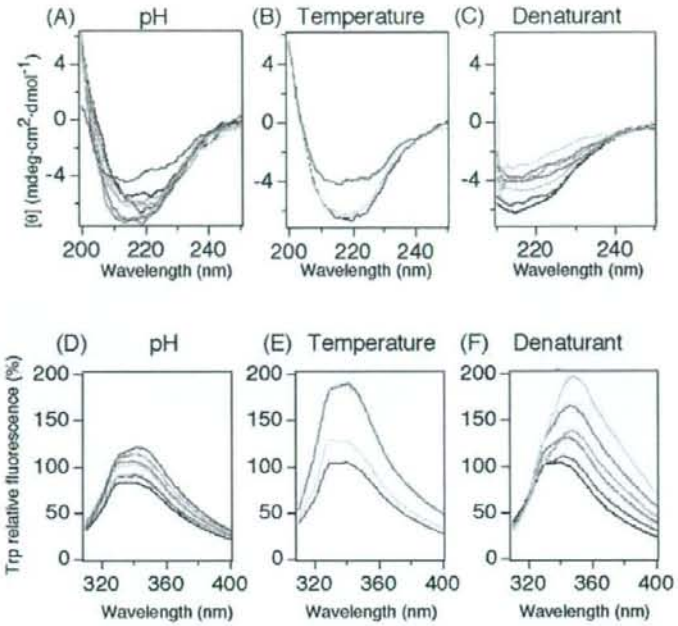

Fig. 2. Secondary and tertiary structural changes. The secondary and tertiary structural changes were detected by CD (A, B, and C) and Trp fluorescence (D, E, and F) spectroscopy. (A) and (D) show the spectra obtained for the pH changes. PrP27–30 (50 *ng/μl*) was incubated in individual pH buffers. Prior to the Trp-fluorescence measurements, the samples were diluted twice with 200 mM Tris-HCl buffer (pH 7.0) to attain a final protein concentration of 25 *ng/μl*. The black, blue, green, yellow, orange, red, grey, and purple lines represent the spectra obtained at pH values of 5.0, 6.0, 7.0, 8.0, 9.0, 10.0, 11.0, and 12.0, respectively. (B) and (E) show the spectra obtained for temperature changes. We incubated 30 and 40 *ng/μl* of PrP27–30 for the CD and Trp-fluorescence experiments, respectively. The blue, yellow, and red lines represent the spectra for the samples treated for 30 min at 25°C, 65°C, and 100°C, respectively. (C) and (F) show the denaturant-dependent spectral changes. PrP27–30 (40 *ng/μl*) was incubated in a buffer containing the indicated denaturant concentration. The black, blue, sky blue, green, red, orange, and yellow lines represent the spectra obtained with 0 M denaturant, 1.0, 2.0, 4.0 M urea, 1.0, 2.0, and 4.0 M GdnHCl, respectively. Relative fluorescent intensity was normalized to that obtained at the wavelength of 345 nm and pH 8.0 at 25°C without denaturant condition (100% folded).

cant increase in solvent-accessible Trp residues.

3) Local conformational changes monitored by ANS and ThT fluorescence: ANS was used to measure the surface hydrophobicity of proteins. ThT was used to detect amyloids. The affinity for ANS was high under acidic conditions, and it reduced under alkaline conditions (Fig. 3A). This result indicated that the surface hydrophobicity of PrP27–30 was increased in acidic conditions but reduced in alkaline conditions. On the other hand, the affinity for ThT was high between pH 8.0 and 9.0, and it reduced under acidic and more alkaline conditions. In particular, the affinity for ThT diminished significantly at pH 12.0, indicating a loss of amyloid structure (Fig. 3D). In contrast, heat treatment did not affect its affinity for ANS (Fig. 3B). The affinity for ThT decreased slightly following treatment at 100°C (Fig. 3E). The ANS signal decreased gradually following an increase in the urea concentration (Fig. 3C, closed squares). However, the ANS fluorescence increased dramatically on treating PrP27–30 with 1.0 M GdnHCl, and it subsequently showed a gradual decrease on treatment with 2.0 and 4.0 M GdnHCl (Fig. 3C, closed circles). The ThT affinity decreased slightly with urea treatment (Fig. 3F, closed squares), while it decreased significantly with GdnHCl treatment (Fig. 3F, closed circles). The GdnHCl treatment reduced the amyloid structure; however, urea did not have a similar effect.

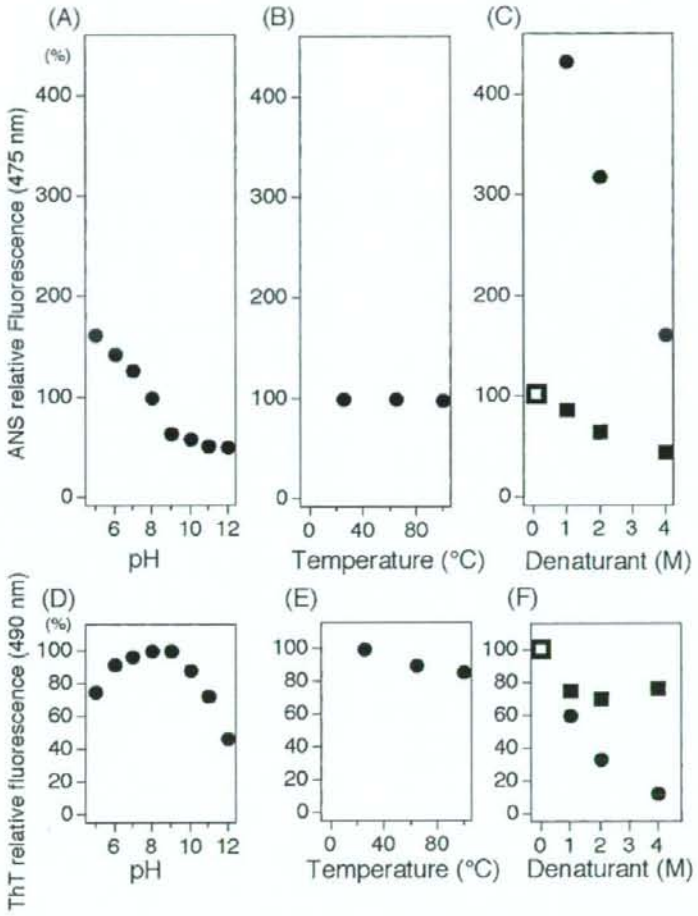

Fig. 3. Local conformational changes in the regions with affinity for ANS and ThT. ANS- (A, B, and C) and ThT- (D, E, and F) fluorescence were monitored at 475 and 490 nm, respectively. The pH-, temperature-, and denaturant concentration-dependent emissions were normalized by the emissions of the samples treated at pH 8.0, at 25°C, and with 0 M denaturant, respectively. We incubated 50 *ng/μl* of PrP27–30 for the pH-dependent experiment, 30 *ng/μl* for the temperature-dependent experiment, and 50 *ng/μl* for the denaturant-dependent experiment. Prior to the ThT-fluorescence measurement, the samples were diluted 20 times with distilled water following treatment with denaturants. The samples treated with urea and Gdn-HCl are represented by closed squares and closed circles, respectively, and the denaturant-untreated sample is represented by an open square. Relative fluorescent intensity was normalized to that obtained at pH 8.0 (A, and D) or at pH 8.5 at 25°C without denaturant condition (B, C, E, and F) (100% folded).

DISCUSSION

The insolubility and aggregative properties of PrP27–30 hinder its structural analysis. In order to prepare small PrP27–30 aggregates, we excluded sarcosyl from the preparation buffer since it exhibits high absorbance in the ultraviolet (UV) region. After sonication under the weak alkaline condition, no visible pellet remained in the purified PrP27–30. We considered that small aggregates of purified PrP27–30 would be dispersed by the sonication and that these could be used in spectroscopic analysis. However, the prepared PrP27–30 remained polymerized; therefore, its molecular

size could not be estimated by size-exclusion chromatography using a Superose 6 10/300 GL column (GE Healthcare Life Science) (data not shown). It has also been reported that the size of CJD prion was greater than 55S [20].

First, we confirmed that further digestion with PK could be used to monitor the conformational alteration of PrP27–30. It has been suggested that the PrP^{Sc} structure, which confers the prion with PK resistance, is inextricably linked with infectivity [3]. Several harsh conditions (treatments at pH 12.0, at 100°C, and with 4.0 M GdnHCl) altered PrP27–30 structure so that it was significantly digested by further PK treatment. These treatments destroy the secondary and tertiary structures of PrP27–30 and render it accessible to PK digestion. Complete loss of prion infectivity was observed on treatment with 4.0 M GdnHCl, consistent with a previous report [3], and a distinct decrease in prion infectivity was observed on alkali treatment at pH 12.0. In contrast, the treatment at 100°C did not effectively destroy its infectivity. These results indicated that the loss of PK resistance is necessary but not sufficient for prion inactivation. Further, we spectroscopically analyzed the differences between infectious- and inactivated-PrP27–30 conformations in solution. The alteration in the secondary and tertiary structures of PrP27–30 in the treatment of pH 12.0, 100°C, 4.0 M urea, and 4.0 M GdnHCl was detected by CD and Trp-fluorescence analysis, respectively. ASN and ThT fluorescence reflect the local structural characteristics of the solvent-accessible hydrophobic regions and the amyloid forms, respectively. Our data demonstrated that the small PrP27–30 aggregates had a β-sheet-rich amyloid structure and solvent-accessible hydrophobic regions under neutral pH conditions. The Trp-fluorescence peak was broad, appearing together with the 2 peaks at 328 and 345 nm. This might be indicative of the coexistence of the solvent-shielded and solvent-accessible Trp residues [9, 10].

It was reported that in the presence of a low concentration of GdnHCl or under acidic conditions, PrP27–30 disassociated into compact intermediates that contained substantial secondary-structure regions, a partially denatured tertiary structure, and multiple high-affinity hydrophobic binding sites for ANS [19]. Treatment with pH 5.0 or 1.0 M GdnHCl demonstrated an increase in the ANS fluorescence together with the presence of substantial β-rich structures (Fig. 2A), and it resembled the previously reported intermediate forms; therefore, our sample facilitated the monitoring of the structural change of PrP27–30 from the native to intermediate and unfolding states in solution.

The results of the unfolding treatment are summarized in Table 2. It revealed that the 3 treatments (pH, heat, and denaturant) caused different structural changes in PrP27–30. The PK resistance of small PrP27–30 aggregates was easily lost by perturbation in the secondary or tertiary structures. The prion inactivation could not be achieved by the loss of PK resistance alone. For a significant loss in prion infectivity, besides perturbation of secondary and tertiary structures, the conformational change in which ThT fluorescence was lost. This implies that denaturation under harsh conditions is necessary to destroy the key structure related to prion infectivity. There is a relationship between the perturbation of the β-sheet-like secondary and tertiary structures of PrP27–30, scrapie amyloid, and infectivity [18]. In contrast, the specific β-sheet-rich structures required for prion infectivity can be differentiated from amyloid formation by Congo red binding [23]. In this study, we indicated that ThT fluorescence might be a good indicator of amyloid formation linked to prion infectivity.

Thus, we demonstrated that the spectroscopic characteristics in PrP27–30 were linked to the prion transmissibility in PrP27–30. This study indicated that the loss of PK resistance was not sufficient, but the significant loss of the amyloid structure of PrP27–30, which was represented by a decrease in the ThT fluorescence, was required for prion inactivation.

ACKNOWLEDGEMENTS. We thank the members of the Prion Disease Research Center in NIAH. This study was supported by a Grant-in-Aid from the BSE Control Project of the Ministry of Agriculture, Forestry and Fisheries of Japan.

REFERENCES

1. Bolton, D. C., McKinley, M. P. and Prusiner, S. B. 1982. Identification of a protein that purifies with the scrapie prion. *Science* **218**: 1309–1311.

Table 2. Summary of the structural changes of small PrP27–30 aggregates

Condition		Secondary structure (CD)	Tertiary structure		Amyloid (ThT)	PK resistance	Infectivity
			Trp	ANS			
pH	5.0	slightly changed	±	++	±	+	+
	12.0	changed	++	–	–	–	±
heat	100°C	changed	+++	+	±	–	+
urea	4.0 M	chnaged	++	–	±	±	+
GdnHCl	4.0 M	highly perturbed	+++	++	–	–	–

–: decrease or loss, ±: slightly decrease, +: not changed , ++: change or increase, +++: significant change or increase.

2. Caughey, B. W., Dong, A., Bhat, K. S., Ernst, D., Hayes, S. F. and Caughey, W. S. 1991. Secondary structure analysis of the scrapie-associated protein PrP27–30 in water by infrared spectroscopy. *Biochemistry* **30**: 7672–7680.
3. Caughey, B., Raymond, G. J., Kocisko, D. A. and Lansbury, P. T. Jr. 1997. Scrapie infectivity correlates with converting activity, protease resistance, and aggregation of scrapie-associated prion protein in guanidine denaturation studies. *J. Virol.* **71**: 4107–4110.
4. Gabizon, R., McKinley, M. P., Groth, D. and Prusiner, S. B. 1988. Immunoaffinity purification and neutralization of scrapie prion infectivity. *Proc. Natl. Acad. Sci. U.S.A.* **85**: 6617–6621.
5. Gasset, M., Baldwin, M. A., Fletterick, R. J. and Prusiner, S. B. 1993. Perturbation of the secondary structure of the scrapie prion protein under conditions that alter infectivity. *Proc. Natl. Acad. Sci. U. S. A.* **90**: 1–5.
6. Greenfield, N. and Fasman, G. D. 1969. Computed circular dichroism spectra for the evaluation of protein conformation. *Biochemistry* **8**: 4108–4116.
7. Hayashi, H., Takata, M., Iwamaru, Y., Ushiki, Y., Kimura, K. M., Tagawa, Y., Shinagawa, M. and Yokoyama, T. 2004. Effect of tissue deterioration on postmortem BSE diagnosis by immunobiochemical detection of an abnormal isoform of prion protein. *J. Vet. Med. Sci.* **66**: 515–520.
8. Hill A, F., Antoniou, M. and Collinge, J. 1999. Protease-resistant prion protein produced *in vitro* lacks detectable infectivity. *J. Gen. Virol.* **80**: 11–14.
9. Khorasanizadeh, S., Peters, I. D., Butt, T. R. and Roder, H. 1993. Folding and stability of a tryptophan-containing mutant of ubiquitin. *Biochemistry* **32**: 7054–7063.
10. Li, X.-M.,Malakhova, M. L., Lin, X., Pike, H. M., Chung, T., Molotkovsky, J. G. and Brown, R. E. 2004. Human glycolipid transfer protein: probing conformation using fluorescence spectroscopy. *Biochemistry* **43**: 10285–10294.
11. McKinley, M. P. and Prusiner, S. B. 1991. Ultrastructural studies of prions. pp.75–91. *In*: Transmissible Spongiform Encephalopathies: Scrapie, BSE and Related Human Disorders, Current Topics in Microbiology and Immunology, 172 (Chesebro, B. W. ed), Springer-Verlag, Berlin.
12. McKinley, M. P., Bolton, D. C. and Prusiner, S. B. 1983. A protease-resistant protein is a structural component of the scrapie prion. *Cell* **35**: 57–62.
13. Oesch, B., Westaway, D., Wälchli, M., McKinley, M. P., Kent, S. B. H., Aebersold, R., Barry, R. A., Tempst, P., Teplow, D. B., Hood, L. E., Prusiner, S. B. and Weissmann, C. 1985. A cellular gene encodes scrapie PrP 27–30 protein. *Cell* **40**: 735–746.
14. Prestrelski, S. J., Arakawa, T. and Carpenter, J. F. 1993. Separation of freezing- and drying- induced denaturation of lyophilized proteins using stress-specific stabilization, II. Structural studies using infrared spectroscopy. *Arch. Biochem. Biophys.* **303**: 465–473.
15. Prusiner, S. B., McKinley, M. P., Bowman, K. A., Bolton, D. C., Bendheim, P. E., Groth, D. F. and Glenner, G. G. 1983. Scrapie prions aggregate to form amyloid-like birefringent rods. *Cell* **35**: 349–358.
16. Prusiner, S. B., Cochran, S. P., Groth, D. H., Downey, D. E., Bowman, K. A. and Martinez, H. M. 1982. Measurement of the scrapie agent using an incubation time interval assay. *Ann. Neurol.* **11**: 353–358.
17. Safar, J., Wang, W., Padgett, M. P., Ceroni, M., Piccardo, P., Zopf, D., Gajdusek, D. C. and Gibbs, C. J. Jr. 1990. Molecular mass, biochemical composition, and physicochemical behavior of the infectious form of the scrapie precursor protein monomer. *Proc. Natl. Acad. Sci. U. S. A.* **87**: 6373–6377.
18. Safar, J., Roller, P. P., Gajdusek, D. C. and Gibbs, C. J. Jr. 1993. Thermal stability and conformational transitions of scrapie amyloid (prion) protein correlate with infectivity. *Protein Sci.* **2**: 2206–2216.
19. Safar, J., Roller, P. P., Gajdusek, D. C. and Gibbs, C. J. Jr. 1994. Scrapie amyloid (prion) protein has the conformational characteristics of an aggregated molten globule folding intermediate. *Biochemistry* **33**: 8375–8383.
20. Sklaviadis, T. K., Manuelidis, L. and Manuelidis, E. E. 1989. Physical properties of the Creutzfeldt-Jakob disease agent. *J. Virol.* **63**: 1212–1222.
21. Spassov, S., Beekes, M. and Naumann, D. 2006. Structural differences between TSEs strains investigated by FT-IR spectroscopy. *Biochim. Biophys. Acta* **1760**: 1138–1149.
22. Takahashi, K., Shinagawa, M., Doi, S., Sasaki, S., Goto, H. and Sato, G. 1986. Purification of scrapie agent from infected animal brains and raising of antibodies to the purified fraction. *Microbiol. Immunol.* **30**: 123–131.
23. Wille, H., Michelitsch, M. D., Guénebaut, V., Supattapone, S., Serban, A., Cohen, F. E., Agard, D. A. and Prusiner, S. B. 2002. Structural studies of the scrapie prion protein by electron crystallography. *Proc. Natl. Acad. Sci. U. S. A.* **99**: 3563–3568.
24. Yokoyama, T., Kimura, K., Tagawa, Y. and Yuasa, N. 1995. Preparation and characterization of antibodies against mouse prion protein (PrP) peptides. *Clin. Diagn. Lab. Immunol.* **2**: 172–176.

A Basic Fibroblast Growth Factor Improves Lower Extremity Wound Healing With a Porcine-Derived Skin Substitute

Sadanori Akita, MD, PhD, Kozo Akino, MD, PhD, Katsumi Tanaka, MD, Kuniaki Anraku, MD, and Akiyoshi Hirano, MD

Background: **Although a number of cytokine or growth factor therapies for wound acceleration have been reported, few mentioned the quality of the outcome. The lower extremity is important in esthetics as well as in function, because it is exposed. Recently, a growth factor, namely basic growth factor (bFGF) is widely used for difficult wound healing with a porcine-derived bilayered artificial dermis for better wound closure. Thus, their combination use was tested clinically.**

Methods: **Sequential lower extremity reconstruction by an artificial dermis with or without bFGF administration and secondary split-thickness skin grafting was measured for hardness using a durometer, and the moisture parameters assessed such as effective contact coefficient, transepidermal water loss (TEWL), water content and thickness using a moisture meter for at least 6 months after the final procedure and compared with normal skin control.**

Results: **There was significantly less skin hardness using a durometer in bFGF treatment compared with non-bFGF treatment (16.2 ± 3.83 vs. 29.2 ± 4.94, $p < 0.01$). Effective contact coefficient, TEWL, water content, and thickness in non-bFGF treatment were all significantly greater than those in bFGF treatment, whereas water content and thickness in bFGF treatment were comparable with those of the control.**

Conclusion: **The use of bFGF as artificial dermis for extensive and deeper tissue loss coverage demonstrated better reconstruction quality in terms of hardness using a durometer and the function of the stratum corneum by moisture analysis.**

Key Words: **Basic fibroblast growth factor, Artificial dermis, Lower extremity tissue defect, Quality of wound healing.**

J Trauma. 2008;64:809–815.

Reconstruction of the lower extremities can be a concern. After extensive soft tissue defects resulting from metabolic changes such as diabetes, atherosclerosis, and subsequent osteomyelitis as well as local infection, contusion, traffic crash, or tumor resection, it is more difficult to resurface skin if the raw surface consists of bone and tendon tissues.[1–4] When insufficient local or systemic nutrient supply such as lower blood perfusion or lower oxygen tension is noted, wound healing deteriorates. Flaps represented by free tissue transfers may be a choice for treatment, but associated medical conditions such as comorbid illness or medications often limit the patients' choice of treatment.[5] Longer and more complicated surgeries may be rejected because of concerns about bleeding or the invasiveness of the surgery, especially in the elderly who might have more complications in the lower extremity during surgery.[6]

Submitted for publication July 6, 2006.
Accepted for publication October 20, 2006.

From the Division of Plastic and Reconstructive Surgery (S.A., K.T., K. Anraku, A.H.), and Division of Anatomy and Neurobiology, Department of Developmental and Reconstructive Medicine (K. Akino), Nagasaki University, Graduate School of Biomedical and Sciences, Nagasaki, Japan.
Supported by grants from the Japanese Ministry of Education, Sports and Culture, #16390511, 16591795, 16791091, 17659562, and 17659563.
Address for reprints: Sadanori Akita, MD, PhD, Department of Plastic and Reconstructive Surgery, Nagasaki University, School of Medicine, 1-7-1 Sakamoto machi, Nagasaki 8528501, Japan; email: akitas@hf.rim.or.jp.

DOI: 10.1097/TA.0b013e31802c8247

To enhance the favorable circumstances for granulation or wound bed preparation for subsequent skin grafting or local flap surgery at wound sites, angiogenic factors such as platelet-derived growth factor-BB and vascular endothelial growth factor are used clinically for irradiated wound healing.[7]

In leg ulcers, there were discrepant expression patterns in the calf of critical limb ischemia between fibroblast growth factor 2 (basic fibroblast growth factor [bFGF]) and vascular endothelial growth factor.[8] Topical administration of platelet-derived growth factor accelerated the healing rate at 20 weeks by 23%[9] and accelerated complete closure by 43% at a maximum of 20 weeks[10] in multicenter-double-blinded, randomized controlled trials. Temporal expression pattern was demonstrated in chronic leg ulcers of hepatocyte growth factor, which may be implicated in accelerated wound healing by exogenous administration,[11] local treatment of chronic leg ulcers by recombinant human granulocyte-macrophage colony-stimulating factor enhanced ulcer healing[12] and further, granulocyte colony-stimulating factor was beneficial in treating diabetic foot ulcer infections in a meta-analysis.[13] Chronic wounds including diabetic ulcers were healed significantly faster by the topical treatment of recombinant bovine bFGF in a randomized, blinded and placebo-controlled clinical trial,[14] whereas no effective results were obtained in topical bFGF treatment for chronic diabetic neuropathic foot ulcers in a randomized controlled pilot trial.[15]

By contrast, fetal or embryonic wound healing has been experimentally and biologically investigated to measure the quality of wounds. Among growth factors, transforming

Table 1 Patient Profiles

	Sex	Age	Location	Size (cm)	Basic Disease
1	M	74	Rt. calf	8 × 5	Osteomyelitis, DM
2	M	30	Lt. lateral malleola, toe	4 × 3 2 × 3	MR, hemodialysis, DM, HT
3	M	82	Bil. calf	5 × 3 4 × 3	TR, fungal infection, HT
4	F	63	Lt. calf	3 × 10	Leg infection, HT
5	M	62	Lt. calf	5 × 3	Osteomyelitis, MI, HT
7	F	72	Lt. calf	10 × 15	DM, HT, ITP, Oral steroids
8	F	21	Lt. calf	6 × 3	Traffic crash
9	M	72	Bil. calf	5 × 4 4 × 2	Low temperature contact burn, DM, HT
10	M	78	Lt. foot	10 × 5	ASO, DM, artythmia
11	F	85	Lt. heel	5 × 2	Osteomyelitis, HT, anemia
12	F	79	Rt. toe	2 × 2	DM, hemodialysis
Average		66.5 ± 20.46			

Rt., right; Lt., left; MR, mitral regurgitation; Bil., bilateral; TR, tricuspid regurgitation; ITP, idiopathic thrombocytopenic purpura; ASO, arteriosclerosis obliterans.

growth factor-β has been extensively investigated and it was concluded that transforming growth factor-β isoforms, and the activity of receptors and modulators might take part in the regulation of scarless or scar-free wound healing.[16–18]

For lower extremity reconstruction of tendon or bone-exposed wounds, an artificial dermis of bilayered collagen sponge and silicone outer membrane complex was beneficial for various anatomic locations including the legs.[19]

Moreover, the combined administration of artificial dermis and growth factor was clinically effective in atypical fingertip burn injuries, soft tissue defects of diabetic feet as well as experimentally in pressure ulcers of a compromised animal model such as genetically diabetic mice.[20–22]

Therefore, we tested the combination of an artificial dermis with the topical administration of bFGF, which is the only angiogenic cytokine currently available in Japan. The bFGF also demonstrated acceleration and improvement in burn wounds in terms of the healing rate and hardness postskin grafting.[23]

PATIENTS AND METHODS

Patients

The subjects were 12 patients (21–85 years old; average 66.5 ± 20.46 years of age, 6 women and 6 men) in this investigation. Lower extremity ulcers were induced by various causes, with underlying diseases such as hypertension (n = 8), diabetes (n = 6), osteomyelitis (n = 3), cardiac valvular insufficiency (n = 2), hemodialysis (n = 2), cellulitis (n = 1), collagen disease (n = 1), and trauma and burn (n = 2). Some patients demonstrated multiple underlying diseases, and therefore the total number exceeds the patient number (n = 12). Patients were compared with those who were previously treated with artificial dermis alone after similar extensive debridement.[24]

The majority of patients in this investigation were elderly. Two cases were younger, patient 2, who was suffering from diabetes and renal failure which required hemodialysis and patient 8, who suffered a traffic crash while traveling in a remote area of Japan and thus the initial therapy was delayed. The size of the wound ranged from 2 × 2 to 50 × 35 cm^2. As comorbid illnesses prevented major surgical interventions such as free flap surgery because of the prolonged operative time, invasiveness and postoperative patient management (Table 1).

Surgical Methods and Artificial Dermis (Pelnac)

Indication of the use of artificial dermis was limited to deep tissue exposure such as tendon, bone or cartilage, which were more difficult in wound closure by skin grafting alone. All surgical debridement was confirmed as sufficiently deep and wide for clinically contaminated or infected lesions. An artificial dermis, a bilayer with an outer silicone membrane and inner porcine tendon-derived collagen sponge (Pelnac, Gunze Co. Ltd, Kyoto, Japan), was immediately applied to all wounds. Except for two cases that did not require secondary skin grafting, another 10 cases underwent secondary split-thickness skin grafting. The average follow-up period after the last procedure, which was either application of the artificial dermis or secondary split skin grafting, was 0.7 ± 0.83 years (0.5 years and 3 years, maximum and minimum, respectively) (Table 2).

Basic Fibroblast Growth Factor (Trafermin, Fiblast Spray)

Genetically recombinant human bFGF was used right after completion of wound bed preparation in the operative ward by spraying. Whereas the artificial dermis was applied before secondary split thickness skin grafting, the bFGF-containing solution was administered from the side of the artificial dermis. The concentration of bFGF was 30 μg of bFGF per 30 cm^2 area as 100 μg of freeze-dried bFGF dissolved in 1 mL of solution of benzalkonium chloride, with

Table 2 Patient Surgical Profiles

	Thickness (inch)	Location	Size (cm)	Follow-Up (yr)	Days to Secondary Skin Grafting
1	0.01	Rt. calf	8 × 5	3	15
2	NA	Toe	2 × 3	0.5	NA
3	0.012	Bil. calf	5 × 3 4 × 3	1.5	16
4	0.01	Lt. calf	3 × 10	3	18
5	0.008	Lt. calf	5 × 3	1	18
6	0.012	Lt. calf	30 × 35	3	14
7	0.007	Lt. calf	10 × 15	1.5	16
8	0.009	Lt. calf	6 × 3	2	19
9	0.01	Bil. calf	5 × 4 4 × 2	1.5	17
10	0.008	Lt. foot	10 × 5	2.5	13
11	0.012	Lt. heel	5 × 2	2.5	14
12	NA	Rt. toe	2 × 2	2	NA
Average	0.01 ± 0.002			0.7 ± 0.83	16.0 ± 2.00

Rt., right; NA, not available because no secondary skin grafting was performed Lt., left; Bil., bilateral.

300 μL sprayed over a 30 cm^2 area with 5 cm distance, and 0.3 mL of such concentration solution was given by this method. Ointment-impregnated gauze was applied to wounds treated with bFGF after waiting for 30 seconds. The bFGF administration continued until secondary skin grafting. The bFGF spray and solution were applied equally to all wounds.

Durometer

The durometer used in this investigation was a TECLOCK GS-701N (TECLOCK, Co., Ltd, Nagano, Japan), which follows the international standard of SRIS 0101 and is defined as a spring instrument to measure hardness, with a 5-mm diameter round noninvasive gauge head, and a value range from 519 to 8379 mN (55–855 gf). The measurement of each point was always perpendicular to the scars and was repeated five times immediately after touching the scar and at 30 seconds after touching, and the mean value of thee adjacent points at least 6 mm apart and 12 mm from the edge of intact skin was assessed at 25°C room temperature and 50% humidity with air conditioning, after the manufacturer's instructions. Informed consent was obtained from all patients and there were no complications or complaints as a result of durometer measurements.[23] Sequential treatment with artificial dermis with or without daily bFGF administration and split skin grafting (bFGF-treated and non-bFGF-treated groups) in the lower extremity was compared in terms of skin hardness.[24] As a normal control, the skin hardness of similar-aged volunteers was investigated at similar anatomic and location points as a normal standard of measurement.

Moisture Meter

A moisture meter (ASA-M2, Asahi Biomed, Co. Ltd, Yokohama, Japan) was used to detect transepidermal water loss (TEWL), water level, and the thickness of the corneal keratinocyte layer of the skin, as well as the effective contact coefficient, determined by electrolytes in the corneal layer. The meter records were used to analyze the susceptibility of conductance using low frequency (160 Hz) alternate currency and detect conductance using high frequency (143 KHz) alternate currency. The proposed formula is as follows:

Skin Conductance (μc) =

Effective Contact Coefficient (%) ×

Water Level (μS).

To enable the use of all these formulary factors, both low frequency and high frequency electric voltages were applied. The round probe of the hand-piece is 5 mm in diameter and detection was set 5 seconds after probe contact with the subject to stabilize electrodes and the skin condition. Each contact point was always perpendicular to the subject and was repeated five times, and the mean value of adjacent points at least 10 mm apart and 20 mm from the intact edge was assessed at 25°C and 50% humidity with air-conditioning, after the manufacturer's instructions. All data were immediately transferred to a personal computer for further analyses. Informed consent was obtained from all patients and there were no complications or complaints as a result of moisture meter measurements. The measurements were performed half a year after healing when the reconstructed areas were evaluated after clinical stabilization.[25] For moisture meter analysis, the same anatomic and location areas of bFGF-treated and non-bFGF-treated groups were compared, and skin moisture meter data of similar-aged volunteers were investigated as a normal standard of measurement.

Statistical Analysis

The results are expressed as the mean ± SD. The data between groups were evaluated by one-way analysis of variance with Bonferroni multiple comparison procedure, and p values <0.05 were considered statistically significant.

RESULTS

Surgical Outcomes

No cases demonstrated wound healing problems. The average days to secondary skin grafting, except in two patients who did not require the procedure, was 16.0 ± 2.00 days and the average thickness of the donor skin was 0.01 ± 0.002 inches, all harvested from the lateral thighs of each patient (Tables 1 and 2). The thickness of the skin graft and the days to secondary skin grafting were very similar to treatment with artificial dermis alone, 17.5 ± 2.00 days and 0.009 ± 0.0022 inches, respectively.[24] There was no problem with blood flow or the local angiogenic environment of these patients, because all cases were ambulatory despite infection or necrosis, but radial debridement deep enough to remove the pathogens was necessary, which required the use of artificial dermis for the coverage of tendons and bones. Thus, comparison of the skin hardness and skin moisture meter parameters was attempted among intact nonsurgical skin, the artificial dermis alone and the bFGF with artificial dermis.

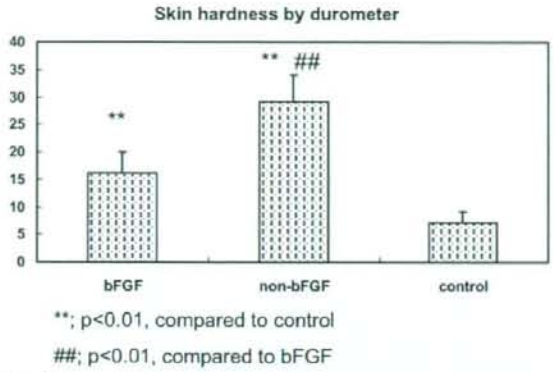

Fig. 1. *The relative value of the durometer reading was compared among groups. The values were 16.2 ± 3.83, 29.2 ± 4.94, and 7.2 ± 2.03, bFGF-treated, non-bFGF-treated and control groups, respectively (p < 0.01 between non-bFGF-treated vs. bFGF-treated and control groups).*

One patient (case 7) had been reconstructed with artificial dermis and subsequent split-thickness skin grafting the previous year in the right extremity, and the other side was reconstructed with bFGF and artificial dermis as bFGF was clinically permitted for use from 2001 in Japan.

Skin Hardness by Duromer

Skin hardness measured using a durometer demonstrated significant differences among groups. The relative value of the actual durometer reading was lowest in the control group, which is nonwounded skin. bFGF treatment together with the artificial dermis was the next lowest and the artificial dermis alone demonstrated the highest value (7.2 ± 2.03, 16.2 ± 3.83, 29.2 ± 4.94, control, bFGF, non-bFGF, respectively, $p < 0.01$) (Fig. 1).

Skin Moisture Analysis

For moisture meter analyses, the effective contact coefficient was significantly higher compared with the nonwounded skin value (control) in both bFGF and non-bFGF-treated artificial dermis groups, and there was a significant difference between bFGF- and non-bFGF-treated groups (10.9% ± 1.05%, 17.9% ± 1.95%, 4.4% ± 0.85%, bFGF, non-bFGF and nonwounded skin (control) groups, respectively, $p < 0.01$). TEWL in the bFGF-treated group was significantly less than that in the non-bFGF group (13.2 ± 2.16 g/m^2/h, 21.2 ± 2.93 g/m^2/h; bFGF treated, non-bFGF treated, respectively, $p < 0.01$). The bFGF-treated group demonstrated a significantly higher TEWL value compared with the control (13.2 ± 2.16 g/m^2/h, 6.3 ± 1.10 g/m^2/h; bFGF treated, control, respectively, $p < 0.01$). The correlation between the effective contact coefficient and TEWL demonstrated significant correlation between the two ($y = 0.81x + 0.053$, $r^2 = 0.86$, $p < 0.01$).

Table 3 Skin Moisture Meter Analysis

	bFGF (n = 12)	Non-bFGF (n = 7)	Non-Wounded (control, n = 20)
Effective contact coefficient (%)	10.9 ± 1.05*	17.9 ± 1.95*†	4.4 ± 0.85
Transepidermal water loss (TEWL) (g/m^2/h)	13.2 ± 2.16*	21.2 ± 2.93*†	6.3 ± 1.10
Water content (μS)	24.7 ± 5.06	46.0 ± 5.67*†	23.5 ± 4.42
Thickness (μm)	12.1 ± 3.14	17.2 ± 1.87*†	10.5 ± 1.62

* $p < 0.01$, compared to control.
† $p < 0.01$, compared to bFGF.

The water content in the non-bFGF group was significantly greater than the bFGF-treated and control groups, whereas there was no significant difference between the bFGF-treated and the control groups (24.7 ± 5.06 μS, 46.0 ± 5.67 μS, 23.5 ± 4.42 μS; bFGF-treated, non-bFGF-treated, control groups, respectively, $p < 0.01$; between control and non-bFGF-treated groups and between bFGF-treated and non-bFGF-treated groups). The thickness of the non-bFGF-treated group was significantly greater than both the control and bFGF-treated groups (12.1 ± 3.14 μm, 17.2 ± 1.87 μm, 10.5 ± 1.62 μm; bFGF-treated, non-bFGF-treated, control groups, respectively, $p < 0.01$) (Table 3). Anatomic locations of the moisture meter and the measurement conditions were similar among three groups.

Case Presentation

An 80-year-old woman was suddenly developed her left calf cellulitis, which caused her emergency debridement of the skin and subcutaneous tissues at Nagasaki University hospital by an orthopedic surgeon on duty. She was then referred to us for further leg reconstruction. There was 1×10^6 CFU/mL of Methicillin-Resistant *Staphylococcus aureus* in wound surface by a swab bacterial culture. Additionally more meticulous debridement including the partial fascia and periosteum in her anterior calf was performed 10 days after initial debridement on her calf and bFGF was sprayed over the wound bed after hemostasis, about 1000 μg of bFGF was sprayed over the wound bed, then an artificial dermis was applied over entire defects. Daily 100 μg of bFGF was needle inserted beneath outer membrane of the artificial dermis. In 2 weeks, 0.012-inch split-thickness skin grafting was placed. In 3 years, a pretibial durometer reading is as low as 18.3, and TEWL demonstrated 23.5 g/m^2/h and thickness of the stratum corneum was 11.5 μm (Fig. 2).

DISCUSSION

Staged lower extremity reconstruction with daily bFGF-treated artificial dermis and subsequently thinner split-thickness skin grafting was beneficial for the quality of reconstructed skin in comparison with the artificial dermis and split-thickness skin grafting alone in terms of hardness and moisture parameters such as TEWL, water content and thickness. The bFGF-

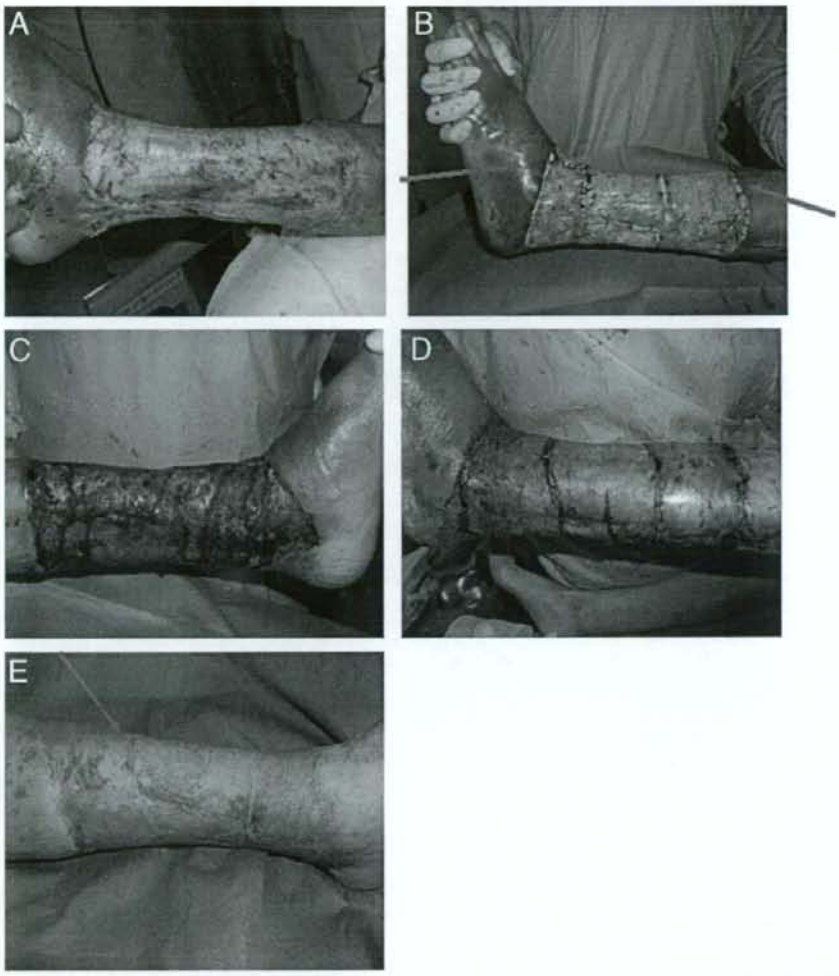

Fig. 2. *An 80-year-old woman suddenly developed calf cellulitis. (A) When she was first referred to us at 10 days after primary debridement by an orthopedic surgeon. (B) After careful hemostasis and 1000 μg of bFGF over the wound bed was sprayed and then an artificial dermis (Pelnac) was covered. From the arrows by needles, total 100 μg of bFGF was administered daily until secondary split-skin grafting. (C) In 14 days after the artificial dermis and daily bFGF application. (D) At time of 0.012-inch split-skin grafting was performed. (E) In 3 years after skin grafting. The pretibial durometer reading demonstrated 18.3 at half a year and 18.5 at 3 years where the periosteum has to be removed.*

treated reconstruction demonstrated almost equal values in water content and thickness, consistent with the softer and thus better nature of the reconstructed lower extremity.

Analysis using a durometer successfully demonstrated a positive correlation with clinical skin hardness severity scores when split-skin grafting was performed with or without bFGF.[23] In this study, there was a significantly high value for non-bFGF artificial dermis reconstruction compared with control (normal skin) and bFGF-treated artificial dermis reconstruction. The relative ratio of a durometer value in the previous skin grafting study was 1:2 (bFGF-treated vs. non-bFGF-treated skin grafting). In staged artificial dermis with or without bFGF-treated skin grafting, it preserved almost the similar ratio, 1:1.8 (bFGF-treated vs. non-bFGF-treated). This may account for how well the primary content of collagen in the artificial dermis sustained applied bFGF in the wound bed and further affected skin remodeling through skin grafting. In fact, there was a report on the possible function of type I collagen as a reservoir of bFGF in a murine model of the subcutis, intramuscular injection, and ischemic hind limb.[26] Analysis using a moisture meter enabled the evaluation of corneal layer (stratum corneum) functions by the

effective contact coefficient, together with TEWL, water content, and layer thickness. Abnormal functioning of corneal layers is well demonstrated in atopic dry skin studies by such as increased TEWL, decreased water content, and increased thickness as the atopic dry skin thickens. As atopic skin decreases the amount of intercellular phospholipids or ceramides, this may account for the damaged function of the corneal layers.[27] In wounded skin, deeper wounds, hypertrophic scars and keloids demonstrated high TEWL and water content values. These data also suggest that proliferative changes in the dermis may affect the corneal layers.

In our study, there was a significantly higher value of TEWL in the non-bFGF-treated group than the bFGF-treated and control groups, and the bFGF-treated group demonstrated significantly higher TEWL than the control. The water content was significantly greater in the non-bFGF-treated group than the control: the bFGF-treated group was comparable with the control and this value was significantly lower than that of the non-bFGF-treated group ($p < 0.01$). bFGF-treated reconstruction may offer better skin remodeling as early as immediately after debridement, which may avoid the development of fibro-proliferative disorders.[28] As the frequency of tape-stripping increases, the water-holding defects of the corneal layers (stratum corneum) are associated with a higher value of TEWL.[29] Thus, TEWL is an important marker of hydration for epithelialization or re-epithelialization after healing. The effective contact coefficient is affected by skin surface electrolytes such as sweating; however, this value also reflects the barrier function of the skin. In our study, there was a correlation between the effective contact coefficient and TEWL. The strongly positive correlation between effective contact coefficient and TEWL demonstrates the higher validity of the moisture measurement. The thickness in both the bFGF-treated and control groups was significantly smaller than that in the non-bFGF-treated group.

Overall, bFGF-treated sequential artificial dermis and skin grafting demonstrated better scarring and well-organized stratum corneum after healing both by durometer and moisture meter analysis.

The advantage of using an artificial dermis includes immediate coverage for deeper tissue exposure such as tendon and bone, protecting from fluid, protein, and electrolyte loss, from microorganism invasion and reducing secondary donor-site morbidity as only thinner skin grafting is required.[19] Also, the combination of artificial dermis with bFGF demonstrated the reconstruction of deep diabetic soft tissue loss,[21] diabetic pressure ulcer healing in a mouse model,[22] and intractable fingertip ulcers caused by burn injury.[20]

Even in larger tissue defects as demonstrated in case 6 of 50×35 cm^2 that are too difficult to cover using the conventional method, or when donor skin is limited, this combination procedure using artificial dermis and bFGF may be useful. In addition, when subsequent or additional debridement is required, donor-site morbidity is minimal and a semi-transparent membrane may be easier to evaluate. The use of a porcine-derived artificial dermis in the lower extremities with daily bFGF administration is easy, safe and useful although secondary split-thickness skin grafting is required and the reconstructed outcome is better in quality.

REFERENCES

1. Henke PK, Blackburn SA, Wainess RW, et al. Osteomyelitis of the foot and toe in adults is a surgical disease: conservative management worsens lower extremity salvage. *Ann Surg.* 2005;241:885–892.
2. Khammash MR, Obeidat KA. Prevalence of ischemia in diabetic foot infection. *World J Surg.* 2003;27:797–799.
3. Patel GK. The role of nutrition in the management of lower extremity wounds. *Int J Low Extrem Wounds.* 2005;4:12–22.
4. Kauffman CA, Lahoda LU, Cederna PS, et al. Use of soleus muscle flaps for coverage of distal third tibial defects. *J Reconstr Microsurg.* 2004;20:593–597.
5. Maloney CT Jr, Wages D, Upton J, et al. Free omental tissue transfer for extremity coverage and revascularization. *Plast Reconstr Surg.* 2003;111:1899–1904.
6. Thomas TA, Taylor SM, Crane MM, et al. An analysis of limb-threatening lower extremity wound complications after 1090 consecutive coronary artery bypass procedures. *Vas Med.* 1999;4:83–88.
7. Hom DB, Manivel JC. Promoting healing with recombinant human platelet-derived growth factor-BB in a previously irradiated problem wound. *Laryngoscope.* 2003;113:1566–1571.
8. Palmer-Kazen U, Wariaro D, Luo F, et al. Vascular endothelial cell growth factor and fibroblast growth factor 2 expression in patients with critical limb ischemia. *J Vasc Surg.* 2004;39:621–628.
9. Steed DL. Clinical evaluation of recombinant human platelet-derived growth factor for the treatment of lower extremity diabetic ulcers. Diabetic Ulcer Study Group. *J Vasc Surg.* 1995;21:71–78.
10. Wieman TJ, Smiell JM, Su Y. Efficacy and safety of a topical gel formulation of recombinant human platelet-derived growth factor-BB (becaplermin) in patients with chronic neuropathic diabetic ulcers. A phase III randomized placebo-controlled double-blind study. *Diabetes Care.* 1998;21:822–827.
11. Nayeri F, Olsson H, Peterson C, et al. Hepatocyte growth factor; expression, concentration and biological activity in chronic leg ulcers. *J Dermatol Sci.* 2005;37:75–85.
12. Bianchi L, Ginebri A, Hagman JH, et al. Local treatment of chronic cutaneous leg ulcers with recombinant human granulocyte-macrophage colony-stimulating factor. *J Eur Acad Dermatol Venereol.* 2002;16:595–598.
13. Cruciani M, Lipsky BA, Mengoli C, et al. Are granulocyte colony-stimulating factors beneficial in treating diabetic foot infections? A meta-analysis. *Diabetes Care.* 2005;28:454–460.
14. Fu X, Shen Z, Guo Z, et al. Healing of chronic cutaneous wounds by topical treatment with basic fibroblast growth factor. *Chin Med J (Engl).* 2002;115:331–335.
15. Richard JL, Parer-Richard C, Daures JP, et al. Effect of topical basic fibroblast growth factor on the healing of chronic diabetic neuropathic ulcer of the foot. A pilot, randomized, double-blind, placebo-controlled study. *Diabetes Care.* 1995;18:64–69.
16. Ferguson MW, O'Kane S. Scar-free healing: from embryonic mechanisms to adult therapeutic intervention. *Philos Trans R Soc Lond B Biol Sci.* 2004;359:839–850.
17. Hsu M, Peled ZM, Chin GS, et al. Ontogeny of expression of transforming growth factor-beta 1 (TGF-beta 1), TGF-beta 3, and TGF-beta receptors I and II in fetal rat fibroblasts and skin. *Plast Reconstr Surg.* 2001;107:1787–1794.
18. Beanes SR, Dang C, Soo C, et al. Down-regulation of decorin, a transforming growth factor-beta modulator, is associated with scarless fetal wound healing. *J Pediatr Surg.* 2001;36:1666–1671.

19. Suzuki S, Kawai K, Ashoori F, et al. Long-term follow-up study of artificial dermis composed of outer silicone layer and inner collagen sponge. *Br J Plast Surg.* 2000;53:659–666.
20. Muneuchi G, Suzuki S, Moriue T, et al. Combined treatment using artificial dermis and basic fibroblast growth factor (bFGF) for intractable fingertip ulcers caused by atypical burn injuries. *Burns.* 2005;31:514–517.
21. Ito K, Ito S, Sekine M, et al. Reconstruction of the soft tissue of a deep diabetic foot wound with artificial dermis and recombinant basic fibroblast growth factor. *Plast Reconstr Surg.* 2005;115:567–572.
22. Kawai K, Suzuki S, Tabata Y, et al. Accelerated wound healing through the incorporation of basic fibroblast growth factor-impregnated gelatin microspheres into artificial dermis using a pressure-induced decubitus ulcer model in genetically diabetic mice. *Br J Plast Surg.* 2005;58:1115–1123.
23. Akita S, Akino K, Imaizumi T, et al. A basic fibroblast growth factor improved the quality of skin grafting in burn patients. *Burns.* 2005;31:855–858.
24. Akita S, Tanaka K, Hirano A. Lower extremity reconstruction after necrotizing fasciitis and necrotic skin lesions using a porcine-derived skin substitute. *J Plast Reconstr Aesthet Surg.* 2006;59:759–763.
25. Akita S, Akino K, Imaizumi T, et al. A polyurethane dressing is beneficial for split-thickness skin-graft donor wound healing. *Burns.* 2006;32:447–451.
26. Kanematsu A, Marui A, Yamamoto S, et al. Type I collagen can function as a reservoir of basic fibroblast growth factor. *J Control Release.* 2004;99:281–292.
27. Imokawa G, Abe A, Jin K, et al. Decrease level of ceramides in stratum corneum of atopic dermatitis. *J Invest Dermatol.* 1991; 96:523–526.
28. Rahban SR, Garner WL. Fibroproliferative scars. *Clin Plast Surg.* 2003;30:77–89.
29. Tagami H, Yoshikuni K. Interrelationship between water-barrier and reservoir functions of pathologic stratum corneum. *Arch Dermatol.* 1985;121:642–625.

Report

Human mesenchymal stem cells may be involved in keloid pathogenesis

Kozo Akino[1], MD, PhD, Sadanori Akita[2], MD, PhD, Aya Yakabe[2], MD, Takao Mineda[3], PhD, Tomayoshi Hayashi[4], MD, PhD, and Akiyoshi Hirano[2], MD

From the [1]Division of Anatomy and Neurobiology, [2]Division of Plastic and Reconstructive Surgery, [3]Division of Oral Cytology and Cell Biology, and [4]Department of Pathology, Nagasaki University, Nagasaki, Japan

Correspondence
Sadanori Akita, MD, PhD
Division of Plastic and Reconstructive Surgery
Department of Developmental and Reconstructive Medicine
Graduate School of Biomedical and Sciences
Nagasaki University
1-7-1 Sakamoto
Nagasaki 852 8501
Japan
E-mail: akitas@hf.rim.or.jp

Abstract

Background The pathogenesis of keloid is poorly understood. Although vigorous investigations have attempted to elucidate the mechanisms or causative factors of keloid, there are little data on why keloids are very intractable and recur easily in each patient.

Methods In an attempt to analyze the possible interaction between human mesenchymal stem cells and keloid-derived fibroblasts, the dual-chamber cell-migration assay, cell proliferation, ultrastructural morphology, and Western blot analysis were used to investigate the production of the extracellular matrices of the coculture.

Results Cell proliferation was not significantly different between keloid-derived fibroblasts and normal dermal fibroblasts during a 4-day observation period. There was a significant cell migration of human mesenchymal stem cells when keloid-derived fibroblasts were placed in the bottom chamber, compared to when normal dermal fibroblasts were placed in the same way in 8-μm diameter pore membranes (190.6 ± 51.45 and 32.0 ± 6.20 cells/field, respectively, $P < 0.01$). With 3-μm diameter pores, the human mesenchymal stem cells migrated in the pores only when the keloid-derived fibroblasts were placed in the bottom chambers (6.4 ± 3.84 cells/field). Monolayer coculture of human mesenchymal stem cells and keloid-derived fibroblasts demonstrated further functional differentiation, such as collagen secretion and abundant rough endoplasmic reticulum. Western blot analysis of the cells in the modified dual-chamber culture demonstrated most significantly abundant fibronectin expression when the human mesenchymal stem cells contained keloid fibroblasts.

Conclusion The results of this study may indicate that human mesenchymal stem cells participate and recruit in keloid pathogenesis by differentiating themselves toward keloid recalcitrant formation and progression.

Introduction

Despite extensive research focused on keloid mechanisms and treatment including the possible involvement of fibrogenic factors, such as transforming growth factor-β (TGF-β),[1] insulin-like growth factor-1 (IGF-1),[2] and platelet-derived growth factor (PDGF),[3] as well as defects in fibrin degradation represented by plasminogen activator inhibitor-1 (PAI-1),[4] little is known on which cell types play a crucial role in the pathogenesis of keloids. While keloid scars recur in individual patients in the same area, some patients develop keloid scars in multiple areas after very minor trauma. Keloid scars are recalcitrant to medical, therapeutic-radiation, or surgical treatments, and they even voluntarily extend over the original wound boundary. There is no fundamental treatment for keloid scars, and the current treatment is by palliative modalities, such as pressure, anti-allergic medication, or steroid injection.[5] Recent developments in stem cell biology have led to the potential application of regenerative medicine by stem cells in the wound-healing process. Among the somatic stem cells, the human bone marrow–derived mesenchymal stem cells (hMSC) are well characterized by surface markers, cell proliferation, differentiation, and regulation.[6] Lipid mediators, such as cysteinyl leukotrienes, are involved in human mesenchymal stem cell differentiation.[7] Keloid fibroblasts significantly enhance the extracellular matrix expression, such as collagen type 1, fibronectin, and PAI-1, under TGF-β and IGF-1 in a dose-dependent manner.[8] Thus, excessive extracellular matrix production from keloid fibroblast is targeted by therapy and pathogenesis. In a mouse model of systemic sclerosis by daily injection of bleomycin, sclerotic cutaneous change was reversed through intravenous administration of antibody against TGF-β[9]; however, detailed information concerning the regulation of

International Journal of Dermatology 2008, 47, 1112–1117